

# Chapter 1

## Quantum Hydrodynamics

Shabbir A. Khan and Michael Bonitz

**Abstract** Quantum plasma physics is a rapidly evolving research field with a very inter-disciplinary scope of potential applications, ranging from nano-scale science in condensed matter to the vast scales of astrophysical objects. The theoretical description of quantum plasmas relies on various approaches, microscopic or macroscopic, some of which have obvious relation to classical plasma models. The appropriate model should, in principle, incorporate the quantum mechanical effects such as diffraction, spin statistics and correlations, operative on the relevant scales. However, first-principle approaches such as quantum Monte Carlo and density functional theory or quantum-statistical methods such as quantum kinetic theory or non-equilibrium Green's functions require substantial theoretical and computational efforts. Therefore, for selected problems, alternative simpler methods have been put forward. In particular, the collective behavior of many-body systems is usually described within a self-consistent scheme of particles and fields on the mean-field level. In classical plasmas, further simplifications are achieved by a transition to hydrodynamic equations. Similar fluid-type descriptions for quantum plasmas have been proposed and widely used in the recent decade. This chapter is devoted to an overview of the main concepts of quantum hydrodynamics (QHD), thereby critically analyzing its validity range and its main limitations. Furthermore, the results of the linearized QHD in unmagnetized and magnetized plasmas and a few nonlinear solutions are examined with illustrations. The basic concepts and formulation of particle-particle interactions are also reviewed at the end, indicating their possible consequences in quantum many-body problems.

---

Shabbir A. Khan  
National Centre for Physics, Quaid-i-Azam University Campus, Islamabad 45320, Pakistan;  
email: sakhan@ncp.edu.pk

Michael Bonitz  
Institut für Theoretische Physik und Astrophysik, Christian-Albrechts Universität zu Kiel, 24098  
Kiel, Germany;  
email: bonitz@physik.uni-kiel.de

## 1.1 Introduction

Conventional plasmas found naturally in the visible universe (e.g., the Sun's environment, interplanetary and intergalactic media, etc.) or created in the laboratory (e.g., discharge experiments, etc.) are ionized gases in which the charged particles (electrons and different ions) move under the influence of long-range electromagnetic forces. Although, the individual particles obey the laws of quantum mechanics, the wave nature of the particles has practically no effect on the collective motion in the case of classical plasmas, due to the large inter-particle distances, and the plasma can adequately be described by classical dynamical laws in the framework of Newtonian mechanics and Maxwell-Boltzmann (MB) statistics.

It has been known since long ago that the conduction electrons in metals behave very similar to gaseous plasmas and can be well treated as an electron gas. Similarly, electrons in semiconductors excited across the band gap behave very similarly to a plasma of electrons (in the conduction band) and holes (missing electrons in the valence band). This electron-hole plasma is very similar to classical two-component plasmas. However, there is a basic difference: the relevant statistics changes from MB to Fermi-Dirac (FD), applicable to identical quantum particles with half-integer spin whose distribution is restricted by the Pauli exclusion principle. The quantum electron gas in metals is globally neutralized by the lattice ions whose properties are governed by various control parameters (see below, for more details, see [1]). Recent developments in ultrafast spectroscopic techniques have made it possible to monitor the collective behavior of the quantum electron gas confined in nanomaterials (nanotubes, metal clusters, nanoparticles, etc.) at the femtosecond scale. The collective electron oscillations which are principally governed by plasma effects lead to fascinating paradigm of plasmonics – a research field currently under way at a breathtaking pace [2, 3, 4, 5]. In semiconductors, even though the electron density is much lower than in metals, the ongoing miniaturization in nanotechnology applications has made the spatial variations of the doping profiles comparable to the de Broglie wavelength of the electrons. This indicates the central role of typical quantum effects, such as tunneling, on the behavior of future electronic components.

Other realizations of quantum plasmas are obtained in high-density matter. By using various dynamic and static compression techniques (diamond anvils, gas guns, and so on), or high energy sources (intense lasers, ion beams), dense plasma conditions with densities of the order of  $10^{23}\text{cm}^{-3} \dots 10^{25}\text{cm}^{-3}$  have been achieved in the laboratory [1]. At the initial stage of compression, the temperature is moderate, and degenerate electrons are expected. Significance of such experiments can be seen in the warm dense matter (WDM) physics – an area getting increasing attention due to its importance for inertial confinement fusion (ICF). The advent of superintense lasers (in the petawatt range and beyond) provides tools for light matter-interactions expecting the creation of overdense plasmas in the laboratory reaching an electron number density up to  $\sim 10^{26}\text{cm}^{-3}$  [6, 7]. Such developments open the door to new avenues, making it possible to understand the physics underlying various phenom-

ena, experimentally probing the quantum plasma regimes and, ultimately exploiting such states for applications.

Ionized quantum matter is found naturally in dense astrophysical objects such as stellar cores, white and brown dwarfs, neutron stars, and interior of giant planets (e.g., Jovian planets) in the solar system [8]. The electrons in these systems constitute a degenerate plasma that often is under extreme conditions of density. Thereby, the electrons may be non-relativistic or relativistic, depending upon the ratio of the Fermi energy to the rest energy of an electron. At extremely high densities, exceeding the nuclear density,  $n$  ( $\sim 10^{39} \text{cm}^{-3}$ ), nuclei break apart (Mott-like transition) giving rise to a dense system of protons and neutrons. At still higher density even protons and neutrons break up, turning into the exotic quark-gluon plasma (QGP), a very special kind of quantum plasma where the particles interact via a (color) Coulomb potential. Such plasmas are believed to having existed immediately after the Big Bang [9], and seen in Relativistic Heavy Ion Collider (RHIC) and Large Hadron Collider (LHC) experiments. For an overview on the density-temperature range, see Fig. 1.1, for a more detailed introduction to quantum plasmas, see Ref. [1].

**Basic parameters.** In many-particle quantum systems, the mean particle distance  $\bar{r}_i = [3n_i/4\pi]^{-1/3}$  of species  $i$  is comparable to or smaller than the de Broglie wavelength associated with the particle,  $\Lambda_{B_i} = h/\sqrt{2\pi m_i k_B T_i}$ , where  $m_i$  is particle mass and  $T_i$  the temperature, leading to an overlap of the wave functions of spatially extended mutually penetrating quantum particles, and the quantum degeneracy parameter exceeds unity,  $\chi_i = n_i \Lambda_{B_i}^3 \geq 1$ . For classical systems, one can define the Coulomb coupling parameter as the ratio of the average interaction energy  $\langle U_{ii} \rangle = (e_i^2/4\pi\epsilon)(1/\bar{r}_i)$  and the average kinetic (thermal) energy  $\langle K \rangle = E_{T_i}$  ( $\sim k_B T_i$ ), i.e.,  $\Gamma_i = |\langle U_{ii} \rangle|/E_{T_i}$ , where  $\epsilon$  is the static background dielectric constant. But, for sufficiently cold and dense plasmas which are quantum degenerate (assuming fermions), i.e.  $\chi_i > 1$ , the role of kinetic energy is taken over by the Fermi energy;  $E_{F_i} = \hbar^2 (3\pi^2 n_i)^{2/3} / 2m_i$ . In a quantum plasma, the strength of particle correlations is measured by the Brueckner parameter;  $r_{si} = \bar{r}_i/a_{B_i}$ , where  $a_{B_i} = (\epsilon/e_i^2)(\hbar^2/m_i)$  is the effective Bohr radius. It is easily verified that  $r_{si} \propto \Gamma_{q_i} = |\langle U_{ii} \rangle|/E_{F_i} = (\hbar\omega_{p_i}/E_{F_i})^2$ , where  $\Gamma_q$  is the quantum generalization of the Coulomb coupling parameter [10], and  $\omega_{p_i}$  is the plasma frequency given by  $\omega_{p_i}^2 = n_i e_i^2 / \epsilon_0 m_i$  for particles in vacuum (in three dimensions). The ideal behavior is recovered for  $\chi_i \ll 1$ ,  $\Gamma_i \ll 1$ , in classical and  $\chi_i \gg 1$ ,  $r_{si} \ll 1$ , in degenerate quantum plasmas. Both these limits correspond to a structureless gas-like system and are simple to analyze theoretically. The quantum coupling parameter shows the peculiar property of dense quantum systems: they become increasingly ideal with increasing density<sup>1</sup>. In contrast, in classical systems, the strength of correlations increases upon compression since the interaction energy increases as  $n^{1/3}$  but thermal energy remains constant. Various plasma regimes are illustrated in the density-temperature phase diagram in the following section.

<sup>1</sup> Note that this is different from ultrarelativistic quantum plasmas where kinetic and interaction energy have the same scaling with density.

**Additional parameters.** For completeness we list further parameters of relevance in quantum plasmas. The Fermi energy is related to a characteristic velocity, wave number and length scale: the Fermi velocity, wave number and wave length,  $v_F^2 = 2E_F/m$ ,  $k_F^2 = 2mE_F/\hbar^2$  and  $\lambda_F = 2\pi/k_F$ . Furthermore, there exists a characteristic screening length - the Thomas-Fermi length  $\lambda_{TF}$  that replaces the Debye screening length of a classical plasma, [ $\lambda_D^2 = k_B T / (2\pi e^2 n)$ ],  $\lambda_{TF} = v_F / (\sqrt{3}\omega_p)$ .

**Theoretical concepts for quantum plasmas.** In quantum plasmas, strong interparticle interactions at de-Broglie length scale impede the use of conventional classical theoretical models. That's why the early descriptions of the most immediate quantum plasma—the quantum electron gas in metals employed different approaches based on semiclassical or quantum mechanical methods including some fundamental works of the pioneers of the field [11, 12, 13, 14, 15, 16]. To find the properties of quantum plasmas obeying FD or Bose-Einstein (BE) statistics, the  $N$ -particle Schrödinger equation is the key equation which describes the evolution of a general pure quantum state arising from some initial state whereas the dynamics of the system is governed by the Hamiltonian. In addition, the solution has to be antisymmetrized for the case of fermions (symmetrized for bosons).

For quantum plasmas, usually the description in terms of mixed states is more appropriate. Then, instead of the wave function, the system is described by the density operator  $\hat{\rho}$ , and the von Neumann equation is the central equation that governs the dynamics of  $\hat{\rho}$ . For many-particle problems, the computational tools based on the (time-dependent) Hartree-Fock (HF, TDHF) method derivable from various techniques [1, 17] provides a useful path which allows for a solution of the many-particle Schrödinger equation in an approximate way, accurately describing and simulating the quantum and spin effects at weak coupling.

If coupling is strong quantum kinetic methods become very demanding. For equilibrium properties a powerful tool is Quantum Monte Carlo, for instance Path Integral Monte Carlo (PIMC) [1, 18, 19]. This method is a very successful first-principle approach avoiding model assumptions, and is well suited for bosonic particles. At the same time, for fermions, it is limited to small systems, due to the so-called fermion sign problem. Equilibrium properties of correlated quantum systems can also be described by quantum molecular dynamics (QMD) techniques which include, for instance, the Wigner function QMD [20], or classical MD with quantum and spin effects included via effective quantum potentials [21]. For equilibrium solutions, theories like the random phase approximation (RPA) and quantum mechanical modeling by density functional theory (DFT) [22, 23] are also very successful. The DFT has a vast range of applicability from atoms, molecules, solids to classical and quantum fluids, and is generalized to deal with many different situations. We further mention ideas to map a quantum system to an effective classical one due to Dharma wardana et al. [24, 25] and Dufty et al. [26, 27, 28].

The standard description of *non-equilibrium* quantum plasmas is based on kinetic theory which involves density matrices or phase space distribution functions of coordinates and momenta. The time evolution of the distribution function is given by a quantum kinetic equation (QKE) which differs from the corresponding classical kinetic equation in the appearance of the explicit difference of arguments in the po-

entials, creating a nonlocal coupling due to finite spatial extension of quantum particles [29]. The self-consistent kinetic modeling is one of the main tools in quantum plasma dynamics in which the notation of phase-space is provided by the Wigner representation in terms of the density matrix. The QKE is a numerically expensive, integro-differential equation which provides the basis for various semiclassical approximations and computational schemes. Furthermore, for non-equilibrium processes, the widely applicable method of non-equilibrium Green's functions (NEGF) has allowed to achieve significant progress in the past few years [29, 30, 31, 32, 33]. It can successfully describe the ultrafast dynamics of many-particle systems and allows for a self-consistent treatment of the collective linear and nonlinear response of correlated Coulomb electron systems and non-perturbative inclusion of external fields and systematic many-body approximations via Feynman diagrams. It also offers an alternative formulation and extension of the TDHF method in terms of a generalized one-particle density matrix  $G(x, t; \bar{x}, \bar{t})$  – the Green's function, which depends upon two space-time variables (in general, also including the spin projection), whose evolution is governed by the Kadanoff-Baym (KB) equations [34]. The KB method has been used to investigate the dielectric properties of plasmon oscillation spectrum with collision effects included in a systematic and consistent way in a correlated electron gas [35]. The developments in analytical and computational tools have led to a number of excellent textbooks including [1, 18, 29, 36] and review articles, for instance [37, 38, 39, 40, 41, 42, 43]. Finally, we mention that the progress is significant, however the solution and detailed analysis of QKE or the full description of many-particle wave functions have been major challenges from a theoretical perspective for the last several decades.

Owing to the analytical complexity of the quantum kinetic approach, drastically simplified macroscopic models (e.g., semiclassical molecular dynamics or quantum hydrodynamics) have been frequently adopted in recent years which can reproduce some of the salient features of quantum plasmas, although not providing the same detailed information which can be extracted from quantum kinetic theory. However, one has a choice with the alternative of studying a physical problem microscopically – with inherent technical difficulties – or macroscopically with a less cluttered and simpler approach which usually has a more restricted applicability range.

Out of the semiclassical approaches for theoretical description of quantum systems, Bohmian quantum mechanics and quantum hydrodynamics (QHD) have been widely used. The former considers real particles in the classical sense of having their configuration space trajectories determined by the Newtonian mechanics with specific positions and momenta (the so-called hidden variables). The latter is a more general method applicable to both pure and mixed states of quantum statistical systems. The QHD equations are usually obtained by taking moments of the appropriate kinetic equation (e.g., the Wigner function equation) in analogy with the moments of the classical kinetic equation. This leads to the conservation laws for particle number, momentum and energy in terms of macroscopic variables by choosing some suitable closure scheme in an approximate way (for details, see below).

Since the early introduction by Madelung [44], various versions of QHD have been developed and applied to many-particle bosonic and fermionic systems, some

of them have been mentioned above. For instance, the QHD equations have been developed to study the dynamics of the quantum electron gas in metals and thin metal films [45, 46, 47, 48, 49]. For electrons in metals, the typical electron density  $n_0 \simeq 10^{23} \text{cm}^{-3}$  yields the quantum coupling parameter  $r_s$  of the order of unity which apparently shows that the collisionless models are not applicable to the metallic electrons. However, the  $e-e$  collision rate (inverse of the electron lifetime  $\tau_{ee}$ ) is controlled by the process of Pauli blocking [46]. At room temperature,  $\tau_{ee} \simeq 10^{-10} \text{s}$  which is much larger than the typical collisionless time scale  $\tau_p$ , the inverse of the electron plasma frequency, i.e.,  $\tau_p = \omega_p^{-1} \simeq 10^{-16} \text{s}$ . In addition, the typical relaxation time scale  $\tau_r \simeq 10^{-14} \text{s}$  is also larger than  $\tau_p$ . Therefore, for time scales smaller than  $\tau_{ee}$ , the electron collisions can be neglected and the collisionless models are appropriate. This standard justification of QHD, however, has to be considered with great caution as it assumes that the electron gas is in thermodynamic equilibrium. For example, laser excited metals with non-equilibrium carrier distributions may have much larger e-e scattering rates, despite the Pauli blocking mechanism.

Similarly, the hydrodynamics formulation is applicable to semiconductors which provides useful explanation of resonant tunneling processes and many ultrafast phenomena at ultrascale scales [50, 51]. The model has also been extended to plasmonics, for instance, surface-plasmon dispersion [52], plasmonic device applications [53], and so on. For low-temperature bosons (e.g., Bose-Einstein condensates (BECs) in trapped Bose gases), the elementary excitations and related phenomena can be seen by employing the Gross-Pitaevskii theory in the spirit of QHD [54, 55]. The model has also been applied to high gain free electron lasers [56], and dense astrophysical plasmas [57], with the possibility of the inclusion of effects like relativity and magnetic fields. However, here as well one has to carefully examine the applicability limits of QHD. Many of the recent predictions of QHD have to be treated with great care as long as no experimental verification is possible or tests against more accurate kinetic approaches have not been made. This has to be reiterated since many of the QHD papers are neglecting these applicability limits and do not provide the necessary tests of their results, see below.

In this chapter, we review the main concepts and limitations of QHD and its validity in various applications starting from the simple case of the weakly coupled, non-relativistic plasma in the electrostatic limit. Since the topic of QHD is not new some obvious derivations are not included and the reader is referred to appropriate references. We start the introduction to the method with a brief note on the initial proposals (Sec. 1.2) and a discussion of the main assumptions and applicability conditions discussing electron and ion plasma waves within linearized QHD. In addition, a brief overview on some nonlinear solutions of QHD as well as results for a magnetized quantum plasma are included with a focus on the relevant low-frequency modes. The basic concepts of correlations and their implications in quantum plasmas are then introduced in Sec. 1.3. Finally, we discuss some recent problems that are related to an incorrect application of QHD to hydrogen bound states and spin effects in dense quantum plasmas. The intention of this chapter is to discuss the concepts in a pedagogical manner giving the interested readers rec-

ommendations for suitable additional references and text books for a more detailed study.

## 1.2 Basics of Quantum Hydrodynamics

The hydrodynamic formulation of systems which demonstrate behavior implicit in quantum mechanical subsystems is almost as old as the Schrödinger equation. It started in the early days of quantum mechanics when Madelung proposed that the Schrödinger equation for spinless one-electron problems can be transformed into the form of hydrodynamics equations. By taking the complex wave function of the form  $\psi = \alpha e^{i\beta}$  with time-dependent, real valued  $\alpha$  and  $\beta$ , he derived the continuity equation and Euler-like equation from the Schrödinger equation. Later on, after a long pause, Bohm and others played a major role in the further developments in this direction. This so-called Madelung hydrodynamics is usually considered as a precursor of the Bohmian mechanics—a quantum theory based on causal interpretation in terms of hidden variables [58, 59, 60] in which the reinterpretation of the solution of the Schrödinger equation and associated phenomena on the lines of classical dynamics was proposed. This interpretation is also known as de Broglie-Bohm theory due to the idea of the pilot-wave by L. de Broglie carried forward by Bohm to its logical conclusion.

### 1.2.1 The time-dependent Schrödinger equation

We begin by writing down the  $N$ -particle Schrödinger equation

$$i\hbar \frac{\partial \Psi_N}{\partial t} = \hat{H}_N \Psi_N, \quad (1.1)$$

$$\hat{H}_N = \sum_{i=1}^N \left\{ -\frac{\hbar^2}{2m} \Delta_i + V(\mathbf{r}_i) \right\}, \quad (1.2)$$

which is supplemented by the initial condition for  $\Psi_0$  for the wave function at  $t = 0$ . In Eq. (1.2),  $\Delta_i$  denotes the Laplace operator (second spatial derivative with respect to the coordinate of particle “i”). The first term in the sum represents the kinetic energy of the particles and  $V(\mathbf{r}_i)$  the potential energy, just like in classical mechanics. Note that in (1.2) we neglect the interaction between the particles. Similarly, we have disregarded the spin variables which will be discussed later.

Now, according to the ideas of Madelung and Bohm, the solution of Eq. (1.1) for time-dependent (in general complex)  $N$ -particle wave function is constructed with the ansatz

$$\Psi_N(\{\mathbf{r}_i\}, t) = A(\{\mathbf{r}_i\}, t) \exp \left[ \frac{i}{\hbar} S(\{\mathbf{r}_i\}, t) \right], \quad \text{where} \quad \{\mathbf{r}_i\} = \{r_1, r_2, \dots, r_N\}, \quad (1.3)$$

with  $A(\{\mathbf{r}_i\}, t)$  being the real amplitude function and  $S(\{\mathbf{r}_i\}, t)$ , the real phase. The statistical distribution of the trajectories determined from  $|\Psi_N|^2$  gives the probability density that the particles are located at the coordinates  $\{\mathbf{r}_i\}$  and thus the measurable physical features of the quantum system just like in classical statistics.

Inserting the ansatz (1.3) for the wave function into the time-dependent Schrödinger equation (1.1) and separating the real and imaginary parts, one obtains the following coupled equations for the two functions  $A$  and  $S$

$$\partial_t S + \sum_{i=1}^N \left[ \frac{1}{2m} (\nabla_{\mathbf{r}_i} S)^2 + V(\mathbf{r}_i) + Q(\{\mathbf{r}_i\}, t) \right] = 0, \quad (1.4)$$

and

$$\partial_t A + \frac{1}{2m} \sum_{i=1}^N [2(\nabla_{\mathbf{r}_i} S) \cdot \nabla_{\mathbf{r}_i} A + A \nabla_{\mathbf{r}_i}^2 S] = 0, \quad (1.5)$$

where, in addition to the conventional potential energy related to  $V(\mathbf{r}_i)$  there arises an new term,  $Q(\{\mathbf{r}_i\}, t)$ , that can be understood as effective *quantum* potential (or Bohm potential) which is absent in the corresponding classical system<sup>2</sup>. Bohm noticed that Eq. (1.5) describes a conservation law of the probability density whereas equation (1.4) has the form of the classical Hamilton-Jacobi equation with the generating function  $S(\{\mathbf{r}_i\}, t)$ , with an additional term given by

$$Q(\{\mathbf{r}_i\}, t) = \frac{\hbar^2}{2m} \frac{\nabla_{\mathbf{r}_i}^2 A}{A}. \quad (1.6)$$

The associated ‘‘effective Hamilton function’’ now contains a total potential that is the sum of the external potential and the quantum potential (summed over all particles) and depends on the dynamical variables  $\{\mathbf{r}_i(t), \mathbf{p}_i(t)\}$  such that the quasi-trajectories may be found from

$$m\dot{\mathbf{r}}_i = \nabla_{\mathbf{r}_i} S(\{\mathbf{r}_i\}, t), \quad (1.7)$$

to yield  $\mathbf{r}_i = \mathbf{r}_i(t)$  with initial position  $\mathbf{r}_0$ , where  $\mathbf{p}_i = \nabla_{\mathbf{r}_i} S(\{\mathbf{r}_i\}, t)$ . The quasi-trajectories evolve under the influence of classical and quantum potentials just like in classical mechanics. The key difference is that the initial state of the particles is, in general, not given in a deterministic manner, but different initial coordinates occur with a finite probability that is given by the initial continuous wave function  $\Psi_0$ . A computational implementation of this scheme then requires a suitable statistical procedure: one has to consider an ensemble of trajectories which start from different initial conditions that have probabilities (statistical weights) according to  $|\Psi_0(\{\mathbf{r}_i\})|^2$ . The resulting time-dependent wave function is then obtained accord-

<sup>2</sup> Note again that the interactions between the particles are neglected, hence all energy contributions are of single-particle type. We will discuss the role of interactions later, in Sec.1.3.



ing to the ensemble average of the individual trajectories with the same weights. The above introduced QHD-description by a well defined wave function can be extended to more general systems within a mixed state representation given by density matrix, for more details, see [29, 61, 62].

Another important remark has to be made. In fact, for a many-particle system (even in a pure state) the Schrödinger equation (1.1) does not provide the correct quantum result. Since quantum particles are either bosons or fermions which differ by their symmetry (in particular, the spin) the  $N$ -particle wave function has to be symmetric (anti-symmetric) for bosons (fermions), i.e. we need to apply a proper (anti-)symmetrization procedure,  $\Psi_N \rightarrow \Psi_N^{A/S}$ , see. e.g. [29, 37, 40]. This has the well-known effect that even noninteracting quantum particles become correlated with each other (or “entangled”). This is fully included in the quantum kinetic methods and simulations that were discussed in the preceding section but is rarely discussed when applying the QHD approach. We will return to this problem below in Sec. 1.4.

### 1.2.2 Quantum mixed state description. Wigner function

In 1932, E. Wigner [63] suggested the phase-space formulation of quantum mechanics, a representation by means of joint distributions of probabilities (more precisely, the quasi-probabilities) for coordinates and momenta in phase space which has led to another route to QHD. Wigner’s original interest was to find quantum corrections to classical statistical theory where the Boltzmann factors contain energies expressible as functions of both coordinates and momenta. The Wigner function doesn’t necessarily stay non-negative in its evolution process for some regions of phase space due to restrictions on the simultaneous measurements of coordinate and momentum by the Heisenberg uncertainty principle. Unlike the classical case, it can therefore not be interpreted as a true probability density. However, it is real, normalizable to unity and gives averages just like the classical statistical distribution function. The Wigner formalism has attracted considerable attention in various disciplines of physics, and has also been the subject of a detailed theoretical analysis, in turn motivating the efforts to formulate various versions of quantum hydrodynamics due to the analogy with classical fluid systems. For more details on quasi-probability distribution functions and Wigner function method, see [10, 29, 64, 65, 66, 67].

The Wigner function is a function of phase space variables  $(\mathbf{r}, \mathbf{v})$  and time (in the following we will use velocities instead of momenta). For simplicity, we consider the one-dimensional problem for quantum statistical mixture of states  $\{\psi_i(x, t), p_i\}$ ,  $i = 1, 2, \dots, K$ , where each wave function  $\psi_i(x, t)$  is assumed with a real non-negative probability  $p_i$  ( $0 \leq p_i \leq 1$ ) satisfying the normalization condition  $\sum_{i=1}^K p_i = 1$ . The results are straightforwardly generalized to higher dimensions. When correlations are ignored, the many-particle wave function can be written as product of one-particle functions. Although we will follow this idea below because it is at the heart of the

QHD approach, one has to clearly realize that this neglects the spin properties of quantum particles. For fermions (or bosons) the  $N$ -particle wave function - even if interactions are neglected - *is not the product of single-particle wave functions* but has the form of a Slater determinant (permanent). Therefore, all QHD results so far assume that the associated exchange corrections (terms additional to the simple product form) are not important. Note that there is no guarantee for that and, depending on the problem studied, the results may be quantitatively or even qualitatively wrong, in particular if spin effects are studied, see Sec. 1.4.

In this way, the quantum mixture (ensemble) of single-particle wave functions is now represented by the density matrix (this is the coordinate representation of a more general quantity – the density operator  $\hat{\rho}$  [33])

$$\rho(x', x'', t) = \sum_{i=1}^K p_i \psi_i(x', t) \psi_i^*(x'', t), \quad (1.8)$$

where  $'^*$  denotes the complex conjugate, and the sum extends over all states contributing to the mixture. The next step is to introduce center of mass and relative coordinates,  $x = (x' + x'')/2$  and  $s = x' - x''$ , respectively which allows to rewrite the original coordinates appearing in Eq. (1.8) as  $x' = x + s/2$  and  $x'' = x - s/2$ . As in classical kinetic theory, these coordinates have different meanings:  $x$  is related to the position of a particle whereas the distance  $s$  is related to the internal structure and is the Fourier adjoint of the momentum<sup>3</sup>. Then, the Wigner function  $f_W(x, v, t)$  can be written as the Fourier transform of (1.8) leading to

$$f_W(x, v, t) = \frac{m}{2\pi\hbar} \sum_{i=1}^K p_i \int_{-\infty}^{\infty} ds \psi_i^*\left(x + \frac{s}{2}, t\right) \psi_i\left(x - \frac{s}{2}, t\right) e^{imvs/\hbar}, \quad (1.9)$$

where  $m$  is the particle mass and  $v = p/m$  is the velocity.

As a side remark we mention that for a general  $N$ -particle system with exchange and correlations described by a statistical mixture we also can compute the single-particle Wigner function. However, then the starting point is the ensemble of the full (anti-)symmetrized  $N$ -particle ensemble wave function  $\Psi_{Ni}^{S/A}(x_1, x_2, \dots, x_N, t)$ . Then the single-particle Wigner function follows from integration over the variable of particles  $2, 3, \dots, N$ ,

$$f_W^{S/A}(x_1, v_1, t) = \int dx_2 dv_2, \dots, dx_N dv_N f_{WN}^{S/A}(x_1, v_1, \dots, x_N, v_N, t), \quad (1.10)$$

where the integrand contains the (anti-)symmetrized  $N$ -particle Wigner function which is the Fourier transform of the (anti-)symmetrized  $N$ -particle density matrix as in the one-particle case above [33]. Instead of the known equation of motion for the  $N$ -particle density matrix – the von Neumann equation – one can also derive a chain of coupled equations for the one-particle, two-particle etc. functions exactly

<sup>3</sup> This is seen by considering a spatially homogeneous system. Then all points  $x$  are equivalent, and the dependence on  $x$  drops out, whereas the dependence on  $s$  remains.

like in the classical case. This hierarchy is nothing but the quantum Bogoliubov-Born-Green-Kirkwood-Yvon (BBGKY) hierarchy of equations [33]. As in the classical case, this hierarchy can only be solved in special cases. In general, one has to resort to closure approximations. In most cases one expresses the two-particle function as a functional of single-particle functions motivated by physical information about the system. The problem is drastically simplified when particle correlations are neglected such that the two-particle Wigner function is approximated as  $f_{W2}^{S/A}(x_1, v_1, x_2, v_2, t) = \Lambda^{S/A}\{f_W(x_1, v_1, t) f_W(x_2, v_2, t)\}$ , where  $\Lambda^{S/A}$  is the (anti)symmetrization operator. If further, exchange (and spin) effects are being neglected we can drop the superscript ‘‘S/A’’, and the two-particle function is just the product of two one-particle functions. This is nothing but the quantum Vlasov (or Hartree) approximation which is commonly used to derive the QHD equations. This approximation means that the quantum plasma is considered as an ensemble of particles interacting through a mean field potential.

The equation of evolution for the one-particle Wigner function (1.9) for a scalar potential  $V$  included in (1.4) is given by

$$\begin{aligned} & \frac{\partial f_W}{\partial t} + v \frac{\partial f_W}{\partial x} \\ & - \frac{im}{2\pi\hbar^2} \int \int ds d\bar{v} e^{im(v-\bar{v})s/\hbar} \left[ V^{\text{eff}}\left(x + \frac{s}{2}\right) - V^{\text{eff}}\left(x - \frac{s}{2}\right) \right] f_W(x, \bar{v}, t) = 0, \end{aligned} \quad (1.11)$$

and is obtained from the Wigner transform (1.9) of the von Neumann equation (or quantum Liouville equation) for the single-particle density matrix [33]. Here,  $V^{\text{eff}} = V + V^{\text{ind}}$  is the total self-consistent potential that contains the mean field potential  $V^{\text{ind}}$  (in the case of Coulomb interaction it is given by the solution of Poisson’s equation) exactly like in the classical Vlasov equation<sup>4</sup>.

The underlying idea is that the quantum transport can be seeded into generalized kinetic equation in the spirit of the Boltzmann equation, appropriately extended with terms that represent quantum corrections. However, the resulting Wigner kinetic equation gives rise to a nonlocal dependence of distribution function on momentum (for details on quantum kinetic equation, see [29]). Due to the finite spatial extension of the quantum particles, the value of the potential energy at one space point also depends on the values of  $V$  at all other points—a pure quantum effect. The classical limit is recovered in the limit of vanishing difference of arguments of the two potentials<sup>5</sup>.

<sup>4</sup> The derivation of Eq. (1.11) follows from straightforward algebra and can be found in many text books, e.g. [29], and will, therefore, not be reproduced here.

<sup>5</sup> Then the integral term becomes  $\frac{1}{m} \frac{dV^{\text{eff}}(x)}{dx} \frac{\partial f_W}{\partial v}$ , as in the classical Vlasov equation.

### 1.2.3 Moments of the Wigner function. Hydrodynamics.

The QHD model [46] can be obtained by taking the moments of (1.11). Since, for all hydrodynamic approaches, the  $j$ -th order moment requires the knowledge of the  $j+1$ -th moment, an infinite chain of equations is found which demands a suitable truncation scheme. Generally, the lower-order moments are related to physically relevant quantities such as the particle density, average velocity, and pressure etc. For mixed states, the pressure tensor (in higher dimensions) requires the second moment of the Wigner function equation to couple to the third moment. The closure assumption allows to establish a relationship between the electron pressure and density demanding an appropriate equation of state. This is, in general, a subtle issue, however, if the system is in thermodynamic equilibrium (or sufficiently close) the known equilibrium results for the equation of state can be used.

Defining the macroscopic variables, i.e., density, mean velocity and pressure in the usual way ( $\sigma_u^2$  is the variance of the velocity):

$$n(x,t) = \int f_W(x,v,t) dv, \quad u(x,t) = \frac{1}{n} \int f_W(x,v,t) v dv, \quad (1.12)$$

$$\frac{1}{m} p(x,t) = \sigma_u^2 = \int f_W(x,v,t) v^2 dv - n(x,t) u^2(x,t) \quad (1.13)$$

and representing each single-particle orbital

$$\psi_i(x,t) = A_i(x,t) \exp(iS_i(x,t)/\hbar), \quad (1.14)$$

with real amplitude  $A_i(x,t)$  and real phase  $S_i(x,t)$ , the first two equations become

$$\frac{\partial n}{\partial t} + \frac{\partial(nu)}{\partial x} = 0, \quad (1.15)$$

$$m \left( \frac{\partial}{\partial t} + u \frac{\partial}{\partial x} \right) u = - \left( \frac{\partial V^{\text{eff}}}{\partial x} + \frac{1}{n} \frac{\partial p}{\partial x} \right), \quad (1.16)$$

where  $V^{\text{eff}} = V + V^{\text{ind}}$  is the single-particle potential<sup>6</sup> and  $p$  is the total scalar pressure which consists of two terms,  $p = p^c + p^q$ , that will be discussed below.

In the following, we consider the simple case of electrons in an electrostatic field where the ions are treated as a homogeneous background. Then  $V^{\text{eff}} = e\phi$  with  $\phi = \phi^{\text{ext}} + \phi^{\text{ind}}$ , which leads from (1.16) to

$$\left( \frac{\partial}{\partial t} + u \frac{\partial}{\partial x} \right) u = \frac{e}{m} \frac{\partial \phi}{\partial x} - \frac{1}{mn} \frac{\partial p^c}{\partial x} - \frac{1}{mn} \frac{\partial p^q}{\partial x}, \quad (1.17)$$

where the induced electrostatic potential  $\phi^{\text{ind}}$  obeys Poisson's equation

<sup>6</sup>  $V$  is in fact non-local, which can be seen from Eq. (1.11), but this is neglected in the hydrodynamic formulation.

$$\frac{\partial^2 \varphi^{ind}(x,t)}{\partial x^2} = \frac{e}{\epsilon_0} \left( \int dv f_W(x,v,t) - n_0 \right), \quad (1.18)$$

with  $\epsilon_0$  and  $n_0$  being the vacuum dielectric constant and uniform background ion density, respectively.

In deriving the above QHD equations for the mean density  $n$  and mean velocity  $u$ , Eq. (1.12), it is now crucial to have a prescription how to connect them with the number density  $n_i(x,t)$  and velocity  $u_i(x,t)$  for each individual orbital. The latter are defined from the wave function (1.14) of each individual orbital according to  $n_i(x,t) = |\psi_i(x,t)|^2 = A_i^2(x,t)$  and  $u_i(x,t) = \partial_x S_i(x,t)/m$ , i.e. just like in the case that the system is in a pure state  $\psi_i$  (as in Madelung's theory). This connection follows readily from the definition of the density matrix (1.8). Thus the average with the Wigner function can be expressed as an ensemble average

$$\langle \dots \rangle = \sum_{i=1}^K p_i \dots \quad (1.19)$$

where the contribution of each orbital enters with the weight  $p_i$ . Thus, for the mean density we obtain

$$n(x,t) = \int dv f_W(x,v,t) = \sum_{i=1}^K p_i \int dv f_{Wi}(x,v,t) = \langle n_i(x,t) \rangle, \quad (1.20)$$

and for the mean velocity follows analogously

$$\begin{aligned} n(x,t)u(x,t) &= \int dv v f_W(x,v,t) = \sum_{i=1}^K p_i \int dv v f_{Wi}(x,v,t) = \\ &= \sum_{i=1}^K p_i n_i(x,t)u_i(x,t) = \langle n_i(x,t)u_i(x,t) \rangle. \end{aligned} \quad (1.21)$$

Finally, we obtain for the pressure from Eq. (1.13) two contributions: the first is the same as in classical hydrodynamics,

$$\frac{p^c(x,t)}{m} = \sigma_u^2 = \sum_{i=1}^K p_i \left( \int dv v^2 f_{Wi}(x,v,t) - n_i(x,t)u_i^2(x,t) \right), \quad (1.22)$$

and is given by the dispersion of the velocities. The orbital densities and velocities will be eliminated from this expression below by postulating a suitable equation of state, see Eq. (1.26).

In contrast to classical hydrodynamics, here appears a second contribution to the pressure that arises from the coordinate dependence of the orbital amplitudes in Eq. (1.14),

$$p^q(x,t) = \frac{\hbar^2}{2m} \sum_{i=1}^K p_i \left[ \left( \frac{\partial A_i}{\partial x} \right)^2 - A_i \frac{\partial^2 A_i}{\partial x^2} \right], \quad (1.23)$$

which has been called *quantum pressure* [46].

Thus the mean values  $n$ ,  $u$ ,  $p^c$  and  $p^q$  can be computed if the wave functions of all orbitals and, hence, the density matrix (Wigner function) are known, which is in general a very difficult task. Instead one can try to get a closed set of hydrodynamic equations, by invoking an equation of state [hydrodynamic closure relation] that relates  $p^c$  and  $p^q$  to the macroscopic density  $n(x,t)$ , thereby eliminating the individual  $n_i$ . In Ref. [46] a very simple solution was proposed: The authors assumed a particular statistical mixture of states in which *all single-electron wave functions (orbitals)  $\psi_i$  have identical amplitudes* that are allowed to be space-dependent, i.e.,  $A_i(x) = A(x)$ ,  $i = 1, \dots, K$ . At the same time the different  $\psi_i$  are allowed to have different phases,  $S_i$ , that are related to the mean orbital velocity  $u_i$  through the relation  $mu_i = \partial S_i / \partial x$  whereas the  $u_i$  are related to the global mean velocity  $u$  via relation (1.21). This condition with the help of (1.9) and (1.13) gives the density  $n = A^2$ . Also, this can be understood as an assumption of uncorrelated electrons where the spatial distribution of each electron defined by the amplitude  $A_i$  doesn't depend upon the spatial distribution of the other electrons in the system [10]. This is a key assumption of QHD for a many-fermion system, and we will discuss and test it more in detail in Sec. 1.2.4.

With this assumption, the relation for  $p^q$  can be rewritten as

$$p^q(n) = \frac{\hbar^2}{2m} \left[ \left( \frac{\partial}{\partial x} \sqrt{n} \right)^2 - \sqrt{n} \frac{\partial^2}{\partial x^2} \sqrt{n} \right], \quad (1.24)$$

where the last term in (1.17) turns out to be

$$\frac{1}{mn} \frac{\partial p^q}{\partial x} = - \frac{\hbar^2}{2m^2} \frac{\partial}{\partial x} \left( \frac{1}{\sqrt{n}} \frac{\partial^2 \sqrt{n}}{\partial x^2} \right). \quad (1.25)$$

When compared to classical fluid equations for electrostatic plasmas, the main difference is the Bohm potential term (1.25) which takes the role of an additional pressure. It is not a true pressure in thermodynamic sense since it involves no velocity averages. In contrast, it is caused by the quantum kinetic energy (which is proportional to minus the Laplacian of the wave function) having the effect of particle spreading (quantum diffraction, tunneling) which is formally equivalent to a positive pressure.

To relate  $p^c$  with the macroscopic density, a useful choice is the equation of state for strongly degenerate (D-dimensional) fermion system in thermodynamic equilibrium (we restrict ourselves to zero-temperature)<sup>7</sup>

$$p^c(x) = p_F^D(n_0) \cdot \left( \frac{n(x)}{n_0} \right)^{5/3}, \quad (1.26)$$

$$p_F^D(n_0) = \frac{2}{D+2} n_0 E_F(n_0) = n_0 \frac{mv_F^2}{D+2}, \quad (1.27)$$

<sup>7</sup> The frequently used notion 'classical' for  $p^c(n)$  is somewhat misleading because it contains  $\hbar$  through  $v_F$ . However it is analogous in the sense of measurement of the velocity dispersion.

where  $v_F = \hbar k_F / m$  is the Fermi velocity defined via the electron Fermi wave number,  $k_F = (3\pi^2 n)^{1/3}$ . Here  $E_F(n_0)$  is the Fermi energy of electrons in a homogeneous system of density  $n_0$ , and  $p_F^D(n_0)$  is the associated Fermi pressure of an ideal Fermi gas at zero temperature. Note that the relation (1.27) between pressure  $p_F^D$  and energy density  $n_0 E_F$  is exact for a non-relativistic ideal Fermi gas at  $T = 0$ . The expression (1.26), on the other hand, extends this result to an inhomogeneous system via the local approximation<sup>8</sup>.

Using the assumption of identical orbital amplitudes, allows to reformulate the quantum hydrodynamic equations (1.15) and (1.17) as a nonlinear Schrödinger (NLS) equation [46]

$$i\hbar \frac{\partial \Psi}{\partial t} = -\frac{\hbar^2}{2m} \frac{\partial^2 \Psi}{\partial x^2} - e\phi\Psi + \tilde{V}\Psi, \quad (1.28)$$

where an effective wave function  $\Psi(x, t) = \sqrt{n(x, t)} \exp(iS(x, t)/\hbar)$  is defined with  $mu(x, t) = \partial S / \partial x$ ,  $n(x, t) = |\Psi|^2$  and  $\tilde{V} = \frac{mv_F^2}{3n_0} |\Psi|^4$ . The nonlinear Schrödinger-Poisson system captures the nonlinear interaction between the electron density fluctuations and the electrostatic potential. The NLS equation is easily amenable to numerical analysis and its generalization can describe the behavior of bosonic systems as well.

A related approach to derive the hydrodynamics equations is based on the Dawson (classical) multistream model [68] which is extended to the quantum case [69] by considering a statistical mixture of  $K$  pure states representing  $K$  “streams” of particles each characterized by the same velocity. Following the Hartree representation (well known in condensed matter physics), the states with wave functions  $\psi_i(x, t)$ ,  $i = 1, \dots, K$  obey  $K$  independent Schrödinger equations that are coupled via the electrostatic potential<sup>9</sup>

$$i\hbar \frac{\partial \psi_i}{\partial t} = -\frac{\hbar^2}{2m} \frac{\partial^2 \psi_i}{\partial x^2} - e\phi\psi_i. \quad i = 1, \dots, K \quad (1.29)$$

Introducing the Madelung representation of wave function (1.14) in (1.29) and separating the real and imaginary parts, it reduces to the hydrodynamic equations, the continuity equation, and an Euler-like equation given by

$$\left( \frac{\partial}{\partial t} + u_i \frac{\partial}{\partial x} \right) u_i = \frac{e}{m} \frac{\partial \phi}{\partial x} + \frac{\hbar^2}{2m^2} \frac{\partial}{\partial x} \left( \frac{\partial^2 \sqrt{n_i} / \partial x^2}{\sqrt{n_i}} \right), \quad (1.30)$$

where  $n_i = A_i^2$ . Setting  $\hbar = 0$ , the classical Dawson relation [68] is retrieved. Although the equation (1.30) takes into account the quantum diffraction effects, its

<sup>8</sup> An alternative choice is a cubic dependence on  $n(x)/n_0$  which is motivated in Ref. [10] by assuming an adiabatic equation of state.

<sup>9</sup> We mention again, that this neglects exchange. Also the picture of “streams” of particles with the same velocity is – strictly speaking – not compatible with the Pauli principle.

limitations are the same as those of (1.17) and are described in the following section.

### 1.2.4 Examples and test of the assumption $A_i(x, t) = A(x, t)$

The assumption that all orbitals have the same space and time-dependent amplitude,  $A_i(x, t) = A(x, t)$ , is a key assumption of QHD for a many-fermion system at zero temperature<sup>10</sup>. It is, therefore, important to verify it. In fact, the single-particle wave functions  $\psi_i$  are often easily found, so it is possible to determine the amplitudes  $A_i$  and phases  $S_i$ , explicitly. We will do this for three typical examples where, for simplicity we consider the one-dimensional case.

**I. Homogeneous free electron gas.** We consider  $N$  particles in a box of length  $2L$  with  $-L \leq x \leq L$ . To model a macroscopic system, periodic boundary conditions are implied, i.e.  $\psi_i(-L) = \psi_i(L)$ , for all  $i$ . If necessary, in the end one can take the limit  $L \rightarrow \infty$  and  $N \rightarrow \infty$ , while maintaining a constant density  $n_0 = N/2L = \text{const}$ . The solutions of the one-particle Schrödinger equation that satisfy these boundary conditions are well known ( $E_l = \hbar^2 k_l^2 / 2m$ ):

$$\begin{aligned} \psi_l(x, t) &= \frac{1}{\sqrt{2L}} e^{-i(E_l t - k_l x)/\hbar}, \quad k_l = lk_0, \quad k_0 = \pi/L, \quad l = \pm 1, \pm 2, \dots \\ A_l(x, t) &= A(x, t) = \frac{1}{\sqrt{2L}} = \text{const}, \quad S_l(x, t) = -E_l t + \hbar k_l x. \end{aligned} \quad (1.31)$$

Evidently, the amplitudes of all orbitals are equal.

**II. Non-interacting electrons in a deep potential well.** Consider now the situation that the electrons are confined to a box of length  $2L$  with  $-L \leq x \leq L$ , where the potential walls are assumed infinitely high. Then the electrons cannot penetrate into the regions  $x < -L$  and  $x > L$  which leads to the boundary condition on the wave functions  $\psi_l(-L, t) = \psi_l(L, t) = 0$ , for all  $l$  and  $t$ . Again, the solutions to this problem are well known from basic quantum mechanics. As usually, the time-dependent solution is  $\psi_l(x, t) = \psi_l(x) e^{-iE_l t/\hbar}$ , where the stationary solution is ( $k_0 = \pi/2L$ )

$$\begin{aligned} \psi_l(x) &= \frac{1}{\sqrt{L}} \cos k_l x, \quad l = \pm 1, \pm 3, \dots, \\ \psi_l(x) &= \frac{1}{\sqrt{L}} \sin k_l x, \quad l = \pm 2, \pm 4, \dots, \\ A_l(x, t) &= \psi_l(x), \quad S_l(x, t) = -E_l t. \end{aligned} \quad (1.32)$$

In this case, the amplitudes  $A_l$  of the orbitals are time-independent, but all completely different, in striking contrast of the main assumption of QHD.

<sup>10</sup> It is also an assumption for a single particle at finite  $T$ .



**III. Non-interacting electrons in a harmonic oscillator potential.** The previous case was characterized by a discontinuous change of the external potential in space. Now we consider the case of a smooth potential that is a quadratic function of the coordinate,  $V(x) = m\omega^2 x^2/2$ . Then, the wave function can extend into the whole space where, due to particle number conservation (normalization condition), it should vanish sufficiently fast for  $|x| \rightarrow \infty$ . The solution is again well known, and the stationary wave functions are given by the Hermite polynomials  $H_l$ ,

$$\begin{aligned} \psi_l(x) &= \frac{1}{\sqrt{2^l l! \sqrt{\pi} x_0}} H_l(u) e^{-\frac{u^2}{2}}, \quad u = \frac{x}{x_0}, \quad x_0 = \sqrt{\frac{\hbar}{m\omega}}, \quad l = 0, 1, 2, \dots \\ A_l(x, t) &= \psi_l(x), \quad S_l(x, t) = -E_l t. \end{aligned} \quad (1.33)$$

As in the second case, the amplitudes of the orbitals are time-independent, but all different.

It is easy to understand the origin of this behavior. In case I the solutions are freely propagating waves described by complex wave functions, and the amplitudes are equal. In contrast, cases II and III correspond to bound states, where the electron motion is spatially restricted. Correspondingly, the stationary wave functions are real<sup>11</sup> and the phases  $S_l$  are just determined by the time-dependent exponential whereas the amplitudes are all different. This also affects the quasi-classical velocities given by  $mu_l = dS_l/dx$ . In case I we obtain  $u_l = \hbar k_l/m$ , whereas in cases II and III  $u_l = 0$  since  $S_l$  is independent of  $x$  for all  $l$ . This is due to the fact, that bound wave functions correspond to standing waves with zero mean momentum.

The most important conclusion of these examples is that the *key assumption of QHD is not fulfilled for spatially confined electrons*. While it is fulfilled for an infinite (noninteracting and spinless) system, this case does never occur in a real plasma. Furthermore, when studying waves in quantum plasmas we are interested in the behavior of electrons in the presence of an external potential well which gives rise to spatial confinement effects. Therefore, the case of confined particles is of particular importance.

It turns out that while the condition of equal orbital amplitudes [10, 66],  $A_l(x, t) = \sqrt{n(x, t)}$ , for all  $l$ , is certainly sufficient for the validity of the QHD equations (together with an appropriate equation of state), it is – most likely – not necessary. In other words, the QHD equations may also be satisfied if the condition  $A_l(x, t) = \sqrt{n(x, t)}$  is not satisfied – which is practically never fulfilled. What is necessary for the QHD equations is that all ensemble averages can be replaced by mean quantities, in particular

$$\frac{2m}{\hbar^2} p^q(x, t) = \left\langle \left( \frac{\partial A_i}{\partial x} \right)^2 - A_i \frac{\partial^2 A_i}{\partial x^2} \right\rangle \Rightarrow \left( \frac{\partial}{\partial x} \sqrt{n} \right)^2 - \sqrt{n} \frac{\partial^2}{\partial x^2} \sqrt{n}, \quad (1.34)$$

<sup>11</sup> This is not universal. For example for Coulomb bound states, the wave function is complex (the angular part).

where  $\langle \dots \rangle$  denotes an average over the orbitals with their weights  $p_i$ . These replacements can be understood as an averaging procedure. Furthermore, note that the terms on the left are rapidly varying in space (at least for the examples II. and III.) because the amplitudes  $A_l$  are oscillating increasingly rapidly with growing  $l$ . This is not the case for the terms on the right, i.e. for the mean density  $n$ . Therefore, these replacements imply a suitable spatial average which – in principle – is consistent with the concept of a hydrodynamic approach. For the example II, an average over the spatial period  $\lambda_l = 2\pi/k_l$  of the square of the amplitude  $A_l^2$  yields  $1/2$ , for all  $l$ . However, problems remain: it is not clear how to systematically choose a *single length scale* averaging over which would apply to *all* (or at least most) orbitals. In some cases, the Thomas-Fermi length  $\lambda_{TF}$ , (or a multiple of it) may be the proper scale as was found e.g. in Ref. [70]. Then for all orbitals with  $\lambda_l \leq \lambda_{TF}$  an averaging occurs with  $A_l^2 \Rightarrow 1/2$ . Furthermore, the validity condition of the assumption (1.34) remains open.

### 1.2.5 Main assumptions and applicability conditions of QHD

The set of equations (1.15), (1.17) and (1.18) constitutes a reduced model whose validity rests on several assumptions, thus imposing important limitations on the model, as described below. In the following we assume that only the electrons are quantum degenerate, so all these conditions apply to the electron component. Generalizations to several quantum components are straightforward.

- (i) The plasma is ideal (weakly coupled) which means all types of interactions (or collision effects) are much weaker than the quantum kinetic energy i.e.

$$r_s \ll 1, \quad \text{or, equivalently,} \quad \Gamma_q \ll 1. \quad (1.35)$$

- (ii) The interaction of the particles is treated in mean field approximation and described by the induced electrostatic potential. No electromagnetic and quantization effects are considered.
- (iii) The wave phase velocities (as well as the particle velocities) are non-relativistic i.e.,  $\omega/k < c$ .
- (iv) The resolvable length scales in QHD are large ( $L > \text{several } \bar{r}$ ) which means the equations are applicable to the long wavelength limit only i.e.,  $\lambda \gg \lambda_{TF}$ , or alternatively  $k \ll \omega_p/v_F$ . Length scales shorter than the Thomas-Fermi screening length  $\lambda_{TF} (= v_F/\sqrt{3}\omega_p)$ , obviously, cannot be resolved. This gives rise to a small parameter<sup>12</sup>,

---

<sup>12</sup> The long wavelength assumption is also evident from analogy with the classical case. The assumption of the classical pressure  $p^c = mn(\langle u_i^2 \rangle - \langle u_i \rangle^2)$  leads to the equation of state,  $p^c = p^c(n)$  for dense degenerate electrons at  $k_B T \ll E_F$ . This in turn demands the condition  $k\lambda_{TF} \ll 1$  to describe the wavelengths within the QHD just like the classical fluid condition  $k\lambda_D \ll 1$  with  $\lambda_D (= k_B T/\sqrt{4\pi n e^2})$  being the Debye length.

$$\kappa \equiv k\lambda_{TF} \ll 1. \quad (1.36)$$

Kinetic phenomena such as Landau damping cannot be described by QHD since they depend on the details of the equilibrium Wigner function and have to be treated with kinetic theory.

- (v) The equation of state of an ideal Fermi gas at  $T = 0$  is used within the local approximation. The extension to space-dependent density profiles is done by introducing a factor  $(n(x)/n_0)^{5/3}$ , cf. Eq. (1.26). This again imposes restrictions on the resolvable length scales. In particular, rapidly varying density profile (e.g. in the case of steep external potentials) cannot be treated properly because the non-locality would give rise to large gradient effects. The zero-temperature assumption requires that  $T \ll T_F$ , otherwise there will be corrections from the Sommerfeld expansion of the Fermi function, e.g. to the equation of state.
- (vi) No energy transport equation is considered. This could be done by taking the second order moment of the Wigner function equation.
- (vii) The model is approximate via the Bohm potential. The closed set of equations follows if the amplitudes  $A_i(x, t)$  of all single-particle orbitals are equal (but not necessarily constant). These orbitals can have different phases  $S_i(x, t)$  which are related to the mean orbital velocity through  $mu_i = \partial S_i / \partial x$ , and  $u_i$  is related to the global mean velocity  $u$  defined in (1.12). This in turn implies the same macroscopic density  $n(x) = A^2(x)$ . A less restrictive condition is given by Eq. (1.34), see the examples and discussion in the previous section.
- (viii) No spin effects are taken into account. However, the inclusion of a magnetic field in QHD is straightforward by starting from a quantum kinetic equation with an electromagnetic field included (by any gauge), as is briefly discussed on the following pages.

As is often the case, a physical model may be valid even beyond its formal conditions of applicability. This is also sometimes the case with QHD which may give reasonable results even beyond the conditions listed above. However, there is no guarantee for this, and a careful analysis of the relevant conditions should always be performed.

In what follows, we have shown in Fig. 1.1 the regions of applicability of the QHD through the density-temperature phase diagram.

The properties of quantum electron gas can be measured with good accuracy in hydrodynamic approximation and provide an ease to search and analyze the linear waves and instabilities which gives insight of the main role of quantum effects.

### ***1.2.6 Linearized QHD: Linear waves of quantum plasmas***

We begin the applications of QHD by considering the linear response of electrons in a quantum plasma to a weak external excitation. Then the QHD equations can be linearized allowing to compute a dielectric function from which the plasmon spectrum is straightforwardly obtained. The problem to study first is electron plasma

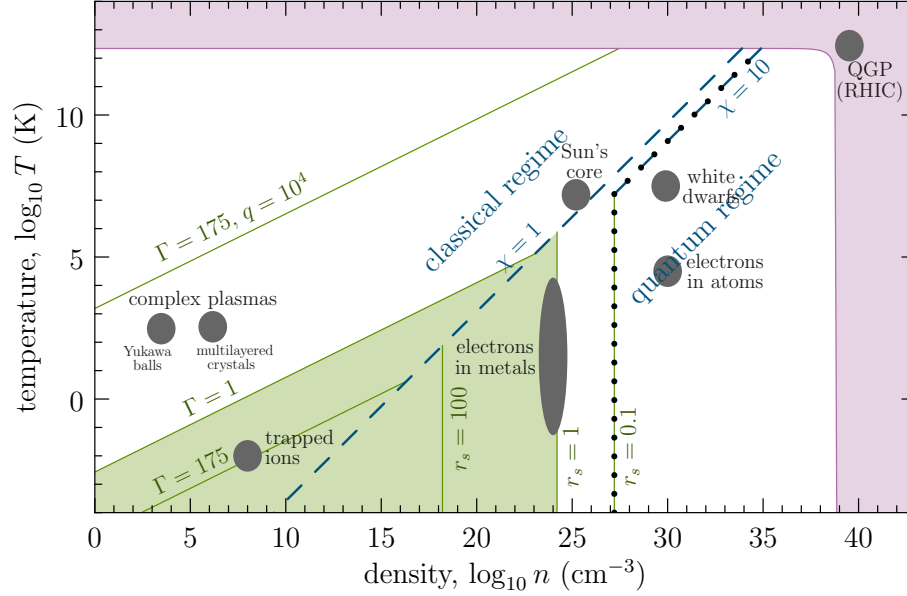


**Fig. 1.1** Density-temperature phase diagram of a one-component plasma, for example electrons in a neutralizing positive background. The green triangle corresponds to strongly correlated electrons, below (left from) the line  $\Gamma = 175$  ( $r_s = 100$ ) electrons form a Wigner crystal. The green line  $\Gamma = 175, q = 10^4$  corresponds to crystallization in dusty plasmas containing particles with charge  $q = 10,000e_0$ . Quantum effects are relevant to the right of the dashed line which is given by  $\chi = 1$ . Some occurrences of quantum plasmas are noted in the figure. QGP denotes the quark-gluon plasma that (is thought to have) existed shortly after the Big Bang and which also was produced at the relativistic heavy ion collider in Brookhaven (RHIC) and at the LHC at CERN. The restriction of QHD to weak coupling,  $r_s < 0.1$ , corresponds to densities larger than  $10^{27} \text{cm}^{-3}$ . The restriction to the ground state ( $T = 0$ ) requires at least  $\chi > 10$ . Note that this makes applications of QHD to electrons in metals or to warm dense matter very questionable. This range is indicated by the dotted line.

oscillations where many results exist against which the QHD result can be directly tested.

### 1.2.6.1 Electron plasma waves

In order to apply the quantum hydrodynamics equations, consider a zero-temperature fermion gas in one spatial dimension with the pressure given by (1.27) as follows

$$p^c(n) = \frac{mv_F^2}{3n_0^2} n^3. \quad (1.37)$$

The electron dynamics are governed by equations (1.15), (1.17)–(1.18) whereas the ions are considered immobile, forming a neutralizing background. Linearizing

the equations around the homogenous equilibrium;  $n = n_0, u = 0$  and  $\varphi = 0$ , and Fourier analyzing as usual with small fluctuating quantities,  $n_1, u_1, \phi_1$ , expressed as  $\exp[i(kx - \omega t)]$ , one obtains the dispersion relation

$$\omega^2 = \omega_p^2 + k^2 v_F^2 + \frac{\hbar^2 k^4}{4m^2} = \omega_p^2 + k^2 v_F^2 \left( 1 + \frac{3}{16} \Gamma_q \kappa^2 \right), \quad (1.38)$$

where  $\omega$  is the wave frequency and  $k$  the wave number. This relation is also derivable from the Poisson-NLS equations (1.18) and (1.28) in the linear limit. While it is nice to keep in the dispersion relation (1.38) the fourth order term in  $k$  one has to clearly remember the limitations of QHD, see above. Indeed, the last equality in (1.38) shows that the  $k^4$  term is about three orders of magnitude smaller (considering that  $\Gamma_q \ll 1$  and  $\kappa \ll 1$ ) than the  $k^2$  term and there is no justification to retain it within QHD.

We now want to compare (1.38) with the result obtained from the Wigner-Poisson model (1.11) and (1.18). Assuming that the potential in (1.11) depends on one coordinate only, say  $x$ , we approximate the equation up to  $O(\hbar^2)$  given by [29]

$$\frac{\partial f_W}{\partial t} + v \frac{\partial f_W}{\partial x} + \frac{e}{m} \frac{\partial \varphi}{\partial x} \frac{\partial f_W}{\partial v} = \frac{e \hbar^2}{24m^3} \frac{\partial^3 \varphi}{\partial x^3} \frac{\partial^3 f_W}{\partial v^3} + O(\hbar^4). \quad (1.39)$$

The right-hand side of (1.39) is due to the non-locality of the potential in the equation for the Wigner function (1.11). It is now easy to see that, in the limit  $\hbar \rightarrow 0$ , one recovers the familiar Vlasov equation for a classical collisionless plasma. The result can be found in perturbation theory and using a Fourier decomposition of the perturbations. Considering the contribution from a monochromatic perturbation proportional to  $\exp[i(kx - \omega t)]$ , i.e.,

$$\begin{aligned} f_W(x, v, t) &= f_0(v) + f_1(v) \exp[i(kx - \omega t)], \\ \varphi(x, t) &= \varphi_1 \exp[i(kx - \omega t)], \end{aligned} \quad (1.40)$$

where  $f_1$  and  $\varphi_1$  are first order perturbed quantities and  $|f_1| \ll f_0$ . It leads to the dispersion relation  $\varepsilon(\omega, k) = 0$ , where the dielectric function  $\varepsilon$  for the Wigner-Poisson system reads<sup>13</sup>,

$$\varepsilon(\omega, k) = 1 - \frac{m \omega_p^2}{n_0 \hbar k^2} \int \frac{f_0(v + \hbar k/2m) - f_0(v - \hbar k/2m)}{kv - \omega} dv. \quad (1.41)$$

With a suitable change of variables<sup>14</sup>, the dispersion relation for high frequency electron plasma oscillations becomes

<sup>13</sup> Here we assume that  $\omega$  contains an infinitely small imaginary part in order to assure causality (Landau pole integration). i.e.  $\varepsilon$  is understood as a retarded quantity.

<sup>14</sup> i.e. changing the integration variable according to  $v \rightarrow v \mp \hbar k/2m$  and bringing both terms to a common denominator.

$$\varepsilon(\omega, k) = 1 - \frac{\omega_p^2}{n_0} \int \frac{f_0(v)}{(\omega - kv)^2 - (\hbar^2 k^4)/4m^2} dv = 0. \quad (1.42)$$

This is just the Lindhard dispersion relation [71] which is well known in solid state physics. In the one-dimensional case, the equilibrium Wigner function for a fully degenerate Fermi gas is given by

$$f_0(v) = \frac{n_0}{2v_F} \quad |v| < v_F, \quad (1.43)$$

$$= 0, \quad |v| > v_F, \quad (1.44)$$

which leads to [29]

$$\varepsilon(\omega, k) = 1 - \frac{m\omega_p^2}{2\hbar k^3 v_F} \ln \left| \frac{\omega^2 - (kv_F - \hbar k^2/2m)^2}{\omega^2 - (kv_F + \hbar k^2/2m)^2} \right| = 0. \quad (1.45)$$

In the long wavelength limit,  $kv_F \ll \omega$ ,  $\hbar k^2/2m \ll \omega$ , expansion of  $\varepsilon(\omega, k)$  in (1.45) gives (1.38), the limit of the kinetic dispersion relation for small wave numbers. Like

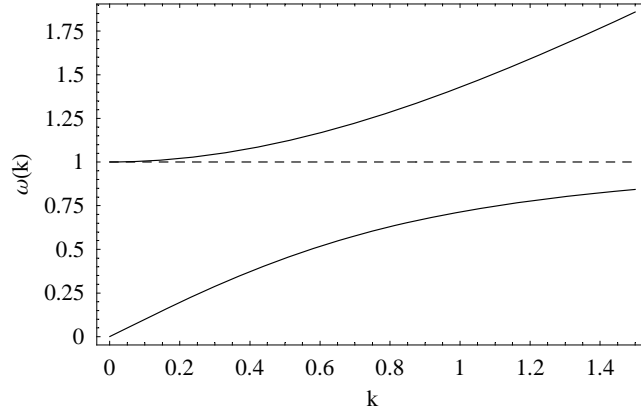


**Fig. 1.2** The dispersion relations (1.38) for electrons (upper curve) and (1.66) for ions (lower curve) are shown for the case of strong degeneracy, ( $E_T \ll E_F$ ). The wave frequency for electrons (ions) is normalized by  $\omega_p(\Omega_p)$  and the wave number by  $\omega_p/v_F(\Omega_p/c_q)$ .

for the one-dimensional case, the equilibrium function equals zero for  $v > v_F$ . Only for smaller velocities  $|v| < v_F$ , the absolute value differs from 1D:  $f_0(\mathbf{v}) = \frac{n_0}{\pi v_F^2}$ , for  $D = 2$ , and  $f_0(\mathbf{v}) = \frac{n_0}{4\pi v_F^3/3}$ , for  $D = 3$ , reflecting the different normalization conditions. So, combining the results for the different dimensions, the dispersion relation for a fully degenerate Fermi gas in the long wavelength limit takes the form

$$\omega^2 = \omega_p^2 + \left( \frac{3}{D+2} \right) k^2 v_F^2 + \frac{\hbar^2 k^4}{4m^2}, \quad (1.46)$$

which should be reproduced by the hydrodynamic equations. Quantum mechanical effects enter this result in two distinct ways: the first is statistical in the sense that the equilibrium distribution is the Fermi distribution, and the second is quantum dynamical [the last term in (1.46)], arising from the energy associated with the finite momentum transfer  $\hbar k$  of an electron interacting with a plasma oscillation<sup>15</sup>.

We note that this type of dispersion of electron plasma oscillations (the quantum Langmuir-like wave as shown in Fig. 1.2) is not new and has already been found by Klimontovich and Silin [12] by using the Wigner distribution function, and by Bohm and Pines [11] by developing canonical transformations of the Hamiltonian of the system of electrons interacting through the electrostatic force.

In analyzing the dispersive properties of quantum plasmas, the coupling and degeneracy parameters play a key role in choosing an appropriate model [72]. The quantum coupling parameter  $r_s$  is a function of density only which shows that the higher is the density of quantum particles, the weaker are the correlations in the system. Some important parameters related to typical degenerate laboratory and astrophysical plasmas are given in the following tables.

**Table 1.1** The parameters of a degenerate electron gas with number densities of the order of metallic electrons with large but constant degeneracy parameter ( $\chi \gg 1$ ).  $E_T = k_B T$ . Since the electron gas is moderately coupled ( $r_s \sim 1$ ), this system is, strictly speaking, not accessible to QHD.

$n$ [ $10^{23} \text{cm}^{-3}$ ]	$\bar{r}$ [ $10^{-9} \text{cm}$ ]	$r_s$	$T$ (K)	$\omega_p$ [ $10^{16} \text{s}^{-1}$ ]	$E_F$ [ $10^{-11} \text{erg}$ ]	$E_T$ [ $10^{-14} \text{erg}$ ]
3.0	9.2	1.10	300	2.4	2.6	4.4
3.7	8.6	1.02	350	2.7	3.0	4.8
4.6	8.0	0.95	400	3.0	3.5	5.5
5.5	7.6	0.90	450	3.3	3.9	6.2
6.5	7.2	0.84	500	3.6	4.3	6.9

The significance of quantum dispersion effects of electron plasma oscillations have been observed in solid-density plasmas. The plasma compression experiments show that the plasmon frequency is a sensitive measure of the electron density and the plasmon dispersion relation includes the Fermi degeneracy effects. In these experiments the temperature is finite and the above result is not applicable. On the other hand, the plasmon dispersion of a classical plasma is well known. It starts from the plasma frequency (for  $k = 0$ ) as well and then  $\omega^2$  increases proportional to  $k^2 v_{th}^2$  [ $v_{th} = (k_B T / m)^{1/2}$  is the electron thermal velocity] – the so-called Bohm-Gross dispersion. If, at finite  $T$ , quantum effects become relevant one obtains the modified

<sup>15</sup> The quantum picture describes this as scattering of an electron with a quantum particle – the plasmon. This momentum change appears in the arguments of the distribution functions in Eq. (1.41). The classical limit is obtained from formally letting  $\hbar \rightarrow 0$ , then the difference of distribution functions turns into a derivative with respect to momentum, and one recovers the classical Vlasov dielectric function.

**Table 1.2** Typical parameter range of a high-density degenerate electron gas found in compact astrophysical systems such as dwarf stars. These systems are weakly coupled and are well suited for a QHD description.

$r_s$	$n$ [ $\text{cm}^{-3}$ ]	$\bar{r}$ [ $10^{-10}\text{cm}$ ]	$E_F$ [erg]	$v_F$ [cm/s]	$\lambda_{TF}$ [ $10^{-8}\text{cm}$ ]
0.10	$4.0 \times 10^{26}$	8.3	$3.1 \times 10^{-9}$	$2.6 \times 10^9$	7.2
0.08	$7.8 \times 10^{26}$	6.7	$4.9 \times 10^{-9}$	$3.2 \times 10^9$	6.5
0.06	$1.8 \times 10^{27}$	5.0	$8.8 \times 10^{-9}$	$4.3 \times 10^9$	5.7
0.04	$6.3 \times 10^{27}$	3.3	$1.9 \times 10^{-8}$	$6.5 \times 10^9$	4.6
0.02	$5.0 \times 10^{28}$	1.6	$7.9 \times 10^{-8}$	$1.3 \times 10^{10}$	3.2

Bohm-Gross relation for small  $k$  that contains quantum corrections [6]:

$$\omega^2 = \omega_p^2 + 3k^2 v_{th}^2 (1 + 0.088n\Lambda_B^3) + \frac{\hbar^2 k^4}{4m^2}, \quad (1.47)$$

where  $\Lambda_B$  is the thermal de Broglie wavelength. Since the degeneracy parameter varies with temperature, the relation shows the increase in wave dispersion with decreasing temperature [Fig. 1.3]. Such noticeable effects of fermion degeneracy in dense matter at relatively high temperature provide useful information about the plasmon dispersion in future experiments, for details, see [6].

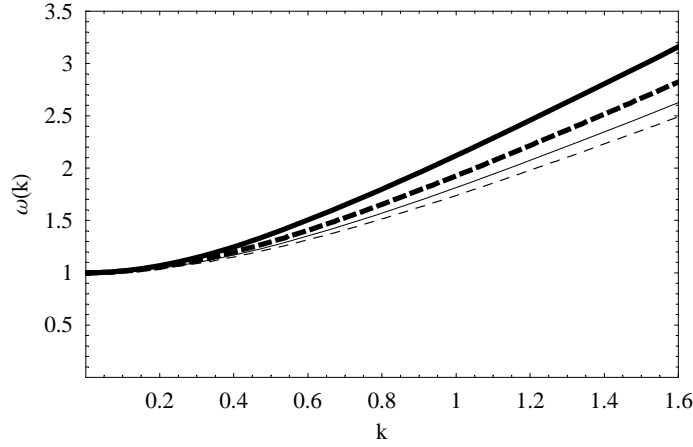


**Fig. 1.3** The modified Bohm-Gross relation (1.47) is shown with variation in degeneracy parameter  $\chi=n\Lambda_B^3$  for a fixed quantum coupling parameter  $r_s = 0.1$ . Thick (thick dashed) line corresponds to  $T = 300K$  ( $T = 500K$ ) whereas thin (thin dashed) line is for  $T = 700K$  ( $T = 900K$ ). The wave frequency is normalized by  $\omega_p$ , and wave number by  $\omega_p/v_F$ , respectively.



### 1.2.6.2 Dielectric tensor of a relativistic quantum plasma

Let us turn to the full dielectric tensor of a degenerate non-relativistic electron gas. This tensor is well known since the 1950s [12, 71] with various generalizations to the fully relativistic quantum regime. The dielectric tensor of an unpolarized isotropic electron–positron plasma can be written as [73, 74]

$$\begin{aligned} \varepsilon_{ij}(\omega, \mathbf{k}) &= \delta_{ij} - \frac{4\pi e^2}{m\omega^2} \int \frac{d^3\mathbf{p}}{\gamma} \frac{\gamma^2 (\omega - \mathbf{k} \cdot \mathbf{v})^2}{\gamma^2 (\omega - \mathbf{k} \cdot \mathbf{v})^2 - Q_r^2} \\ &\times \left[ \delta_{ij} + \frac{k_i v_j + k_j v_i}{(\omega - \mathbf{k} \cdot \mathbf{v})} + \frac{(k^2 - \omega^2/c^2) v_i v_j}{(\omega - \mathbf{k} \cdot \mathbf{v})^2} \right] f(\mathbf{p}), \end{aligned} \quad (1.48)$$

where  $\mathbf{p} = \gamma m \mathbf{v}$ ,  $\gamma = (1 - v^2/c^2)^{-1/2}$ , and  $f(\mathbf{p}) = 2\bar{n}(\mathbf{p}) / (2\pi\hbar)^3$  with  $\bar{n}(\mathbf{p})$  being the sum of the occupation numbers for electrons and positrons and

$$Q_r = \frac{\hbar}{2m} \left( \frac{\omega^2}{c^2} - k^2 \right). \quad (1.49)$$

It is instructive to consider the first denominator of the integrand in Eq. (1.48) the zeroes of which contain the resonance condition for the interaction of electrons (positrons) with the electromagnetic wave:

$$\gamma^2 (\omega - \mathbf{k} \cdot \mathbf{v})^2 - Q_r^2 = [\gamma(\omega - \mathbf{k} \cdot \mathbf{v}) + Q_r][\gamma(\omega - \mathbf{k} \cdot \mathbf{v}) - Q_r]. \quad (1.50)$$

Even though the electromagnetic field is treated classically the zeroes of the two factors can be understood as arising from the emission and absorption of a field quantum by the particles. Thereby the particle energy and momentum change from  $E$  to  $\acute{E}$  and  $\mathbf{p}$  to  $\acute{\mathbf{p}}$  by the discrete amount of  $\hbar\omega$  and  $\hbar\mathbf{k}$ , respectively, i.e.  $\acute{E} = E \mp \hbar\omega$  and  $\acute{\mathbf{p}} = \mathbf{p} \mp \hbar\mathbf{k}$ , where  $E^2 = \mathbf{p}^2 c^2 + m^2 c^4$  and  $\acute{E}^2 = \acute{\mathbf{p}}^2 c^2 + m^2 c^4$ . For non-relativistic particle velocities ( $\gamma \approx 1$ ), the resonance condition (1.50) becomes

$$\omega - \mathbf{k} \cdot \mathbf{v} \mp \frac{\hbar}{2m} \left( \frac{\omega^2}{c^2} - k^2 \right) = 0. \quad (1.51)$$

There other interesting limit is the classical limit. Then the resonance condition (Cherenkov condition) is simply  $\omega - \mathbf{k} \cdot \mathbf{v} = 0$ . Clearly, this limit is recovered by putting  $Q_r \rightarrow 0$  which amounts to neglecting quantum effects (terms proportional to  $\hbar$ ). The quantum correction  $Q_r$  to the classical case is frequently called “quantum recoil” [74] although this is slightly misleading<sup>16</sup>

It is important to note that in a strictly non-relativistic treatment, where one uses the dispersions  $E = \mathbf{p}^2/2m$ , the term  $\omega^2/c^2$  doesn’t appear in the expressions (1.49) and (1.51), showing that a non-relativistic treatment is valid only for  $\omega^2 \ll \mathbf{k}^2 c^2 -$

<sup>16</sup> The energy and momentum balance that includes the absorption and emission of photons has been written above and does not contain any additional “recoil” contribution.

a fact that is well-known in the theory of plasma oscillations but still often ignored, see e.g. Ref. [74]. From Eq. (1.48), the dispersion relation for longitudinal electron waves can be found as before from vanishing of the longitudinal part of the tensor,  $\varepsilon_{ij}(\omega, \mathbf{k}) = 0$ .

**Damping of plasma waves.** The use of QHD neglects certain kinetic effects such as Landau damping. This effect is easily treated taking into account that the dielectric function, Eq. (1.42), is complex since it includes a small imaginary correction to the frequency (see footnote above). So far we did only consider its real part.

In general, the poles at  $v = \omega/k \pm \hbar k/2m$  have both a real and an imaginary part, so the integration has to be performed using the Landau pole integration in the complex velocity plain (analytic continuation is assumed [29]),

$$\varepsilon(\omega, k) = 1 - \frac{m\omega_p^2}{n_0\hbar k^2} \left[ \int_{C_+} \frac{f_0(v)}{k(v - \hbar k/2m) - \omega} dv - \int_{C_-} \frac{f_0(v)}{k(v + \hbar k/2m) - \omega} dv \right] = 0, \quad (1.52)$$

where the integration is performed with Landau contours  $C_{\pm}$  passing under the poles at  $v = \omega/k \pm \hbar k/2m$ . Equation (1.52) is a useful starting point for the discussion of the quantum Landau damping just like the collisionless damping in classical plasmas [13, 49]. Adopting the procedure similar to the classical plasmas, and assuming small damping (or growth) rate  $|\omega_i| \ll \omega$ , we obtain [4, 29]

$$\omega_i = \frac{\pi\omega_p^3}{4n_0k^2} \left[ \frac{f_0(\omega/k + \hbar k/2m) - f_0(\omega/k - \hbar k/2m)}{\hbar k/2m} \right]. \quad (1.53)$$

In the limit  $\hbar \rightarrow 0$ , the known classical relation is recovered,

$$\omega_i = \frac{\pi\omega_p^3}{2n_0k^2} \left. \frac{df_0}{dv} \right|_{v=\omega/k}, \quad (1.54)$$

which shows that (1.53) can be considered as a finite-difference generalization of the classical expression (1.54).

Generalizing (1.52) to three dimensions, the dispersion equation becomes

$$\varepsilon = 1 - \frac{m\omega_p^2}{n_0\hbar k^2} \left[ \int_{C_+} \frac{f_0(\mathbf{v})}{k(v_z - \hbar k/2m) - \omega} d\mathbf{v} - \int_{C_-} \frac{f_0(\mathbf{v})}{k(v_z + \hbar k/2m) - \omega} d\mathbf{v} \right] = 0, \quad (1.55)$$

where  $f_0(\mathbf{v})$  is the equilibrium Wigner distribution function, the Landau contours are passing below the poles lying at  $v_z = \omega/k \pm \hbar k/(2m)$ , and the coordinate system is chosen such that the wave vector points in  $z$ -direction,  $\mathbf{k} = (0, 0, k)$ . Introducing  $f_{0z}(v_z) = \int dv_x dv_y f_0(\mathbf{v})$ , Eq. (1.55) can be integrated over the perpendicular velocity components, leading to

$$\varepsilon = 1 - \frac{m\omega_p^2}{n_0\hbar k^2} \left[ \int_{C_+} \frac{f_0(v_z)}{k(v_z - \hbar k/2m) - \omega} dv_z - \int_{C_-} \frac{f_0(v_z)}{k(v_z + \hbar k/2m) - \omega} dv_z \right] = 0. \quad (1.56)$$

This result is formally the same as (1.52), which allows one to write for the damping/growth rate in the classical limit, analogous to (1.54),

$$\omega_i = \frac{\pi\omega_p^3}{2n_0k^2} \left. \frac{df_{0z}}{dv_z} \right|_{v_z=\omega/k}. \quad (1.57)$$

Damping or growth depend on the sign of the derivative of the projected equilibrium Wigner function. In equilibrium, the distribution function is monotonically decaying with momentum and  $\omega_i$  is negative, corresponding to damping of the wave. In non-equilibrium, the situation can be opposite.<sup>17</sup>

To apply the above result to a degenerate plasma, it is useful to start from the finite-temperature case because the zero-temperature distribution has a singular derivative. Therefore, consider the Thomas-Fermi distribution [76]

$$f_0(\mathbf{v}) = \frac{\alpha}{\exp\left[\beta\left(\frac{mv^2}{2} - \mu\right) + 1\right]}, \quad (1.58)$$

where  $v^2 = v_x^2 + v_y^2 + v_z^2$ ,  $\beta = (k_B T)^{-1}$ , and the normalization constant  $\alpha = 2(m/2\pi\hbar)^3$ . When the temperature  $T$  approaches zero,  $\mu$  approaches to the Fermi energy  $E_F = mv_F^2/2$ . Then the integration over the perpendicular velocity components leads to

$$f_{0z}(v_z) = \frac{2\pi\alpha}{m\beta} \ln \left[ 1 + \exp \left[ \beta \left( \mu - \frac{mv_z^2}{2} \right) \right] \right], \quad (1.59)$$

which has a bell shaped profile. Then, by employing (1.57) for the damping, we obtain

$$\omega_i = \frac{\pi^2\alpha\omega_p^4}{n_0k^3} \left[ 1 + \exp \left[ \beta \left( \frac{m\omega_p^2}{2k^2} - \mu \right) \right] \right]^{-1}, \quad (1.60)$$

where in deriving (1.60), the replacement  $\omega \simeq \omega_p$  was done. Upon analyzing (1.60), we can see that for very low temperature (large  $\beta$ ),  $\mu \simeq E_F$ . Then for  $\omega_p/k > v_F$ , there will be no damping because the wave phase velocity lies in a region where there are no particles. Therefore, high-frequency electron plasma oscillations of a degenerate plasma at very low temperature remain undamped (in the absence of particle collisions [77]). On the other hand, when  $\omega_p/k < v_F$ , the exponential term in (1.60) becomes zero for very large  $\beta$  and damping is significant<sup>18</sup> which cannot be taken into account in the QHD description. So the long wavelength assump-

<sup>17</sup> Note that the existence of instabilities depends on the system dimensionality. While a monotonic increase of  $f_0$  leads to an instability in a one-dimensional and two-dimensional system, this is not the case in a spherically symmetric 3D system [75].

<sup>18</sup> The region where the imaginary part of the dielectric function is non-zero and damping occurs at  $T = 0$  is called "pair continuum" since in this region the plasma wave loses energy by processes where electron-hole pairs are created even when no collisions are taken into account, see e.g. [29]. At finite temperature, there always exist particles with high velocity, so the damping is always non-zero.

tion ( $\omega_p/k > v_F$ ) must hold in the QHD application to degenerate plasmas to avoid damping of waves.

### 1.2.6.3 Streaming instabilities

Considering the one-stream plasma case with a single pure quantum state<sup>19</sup> with equilibrium solutions  $n = n_0$  and  $u = u_0$  at  $\varphi = 0$ , the Fourier decomposition of the perturbed quantities in (1.15), (1.18) and (1.30) leads to the dielectric function

$$\varepsilon(\omega, k) = 1 - \frac{\omega_p^2}{(\omega - ku_0)^2 - \hbar^2 k^4 / 4m^2}, \quad (1.61)$$

where the term  $ku_0$  just represents a Doppler shift and  $v_F \ll u_0$  is assumed. Charge neutrality is provided by the motionless background ions. Here, the frequency  $\omega$  is always real, and the oscillations are stable and undamped [69]. If the effect of quantum statistics is included in the momentum equation, the dielectric function changes to

$$\varepsilon(\omega, k) = 1 - \frac{\omega_p^2}{(\omega - ku_0)^2 - k^2 v_F^2 - \hbar^2 k^4 / 4m^2}. \quad (1.62)$$

When two counter-streaming beams of electrons are considered at equilibrium with streaming velocities  $\pm u_0$  such that  $u_1 = -u_2 = u_0$ ,  $n_1 = n_2 = n_0/2$ , and  $\varphi = 0$ , the dielectric function becomes

$$\varepsilon(\omega, k) = 1 - \sum_{a=\pm 1} \frac{\omega_p^2/2}{(\omega - aku_0)^2 - k^2 v_F^2 - \hbar^2 k^4 / 4m^2}, \quad (1.63)$$

which shows a Doppler shifted spectrum [46] where the dispersion relation is obtained from  $\varepsilon(\omega, k) = 0$ . When the solution for  $\omega^2$  is obtained, two branches are found, one of which is always positive giving stable oscillations. The other solution is negative ( $\omega^2 < 0$ ) which shows

$$[F^2 K^2 - 4(1 - u_F^2)] [F^2 K^4 - 4(1 - u_F^2) K^2 + 4] < 0, \quad (1.64)$$

where the rescaled variables are  $F = \hbar\omega_p/mu_0^2$ ,  $K = ku_0/\omega_p$ , and  $u_F = v_F/u_0$ . For  $u_F < 1$ , a bifurcation in (1.64) is seen for  $F = 1 - u_F^2$ . If  $F \geq 1 - u_F^2$ , the second factor of the inequality is always positive for  $F^2 K^2 < 4(1 - u_F^2)$  which gives rise to an instability. Similarly, if  $F < 1 - u_F^2$ , instability occurs if either  $0 < F^2 K^2 < 2(1 - u_F^2) - 2\sqrt{(1 - u_F^2) - F^2}$ , or  $2(1 - u_F^2) - 2\sqrt{(1 - u_F^2) - F^2} < F^2 K^2 < 2(1 - u_F^2)$ . The limit  $\hbar \rightarrow 0$  leads to  $K^2 < 1$  which is the classical instability

<sup>19</sup> Recall that the Pauli principle prohibits that several electrons move with exactly the same velocity. In reality even in an electron beam the particles have a finite velocity spread  $\Delta v$ , and the present model is to be understood as the limit of small velocity spread,  $\Delta v/u_0 \ll 1$ .

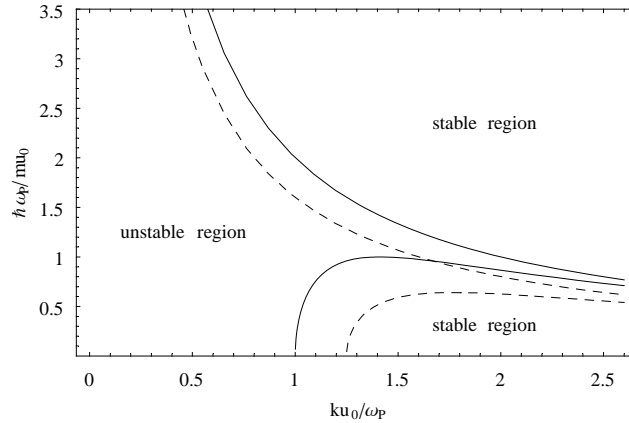


**Fig. 1.4** Two-stream instability analysis in a quantum plasma by using normalized parameters. The area enclosed by the solid curves along the vertical axis shows an unstable region when  $u_F = 0$ . With increase in  $u_F$ , the region shows a shifting as seen by the dashed lines corresponding to  $u_F = 0.6$ .

criterion. The stability/instability region can be seen in Fig. 1.4 with a shift in the presence of nonzero Fermi velocity.

The one and two stream cases show the main features of the oscillation spectrum. However, when generalized to a larger number of streams, the velocity spread, the coherence and resonant contribution as well as collision between the groups of particles lead to additional damping or dephasing, and a kinetic treatment is required.

#### 1.2.6.4 Longitudinal ion waves

When dealing with electrostatic oscillations having a frequency close to the electron plasma frequency, the response of the ion motion is very weak and does not need to be taken into account.

That's why, the ions were considered motionless in the previous section, forming a neutralizing background. However, when the wave frequency is less than the ion plasma frequency,  $\Omega_p = (m/M)^{1/2}\omega_p$ , the dynamics of both species have to be taken into account [ $M$  is the ionic mass]. In a completely degenerate two-component electron-ion quantum plasma, the Fermi energy of the lighter species (electron) is larger than that of the ions due to smaller electron mass,  $E_F \sim m^{-1}$ . Similarly, the de Broglie wavelength scales as  $m^{-1/2}$  and the degeneracy parameter as  $\chi \sim m^{-3/2}$ , thus the ion degeneracy is much smaller than the one of the electrons. So, we will continue to consider the ions classical.

In the case of classical plasmas, the longitudinal ion oscillations give rise to the low-frequency ion-acoustic wave which is modified in quantum plasmas, and a quantum ion-acoustic mode appears [78]. The wave dispersion relation of longitudinal ion waves in homogenous electron-ion plasmas is given by the zeroes of the

longitudinal dielectric function,

$$1 + \chi_e^{lo}(\mathbf{k}, \omega) + \chi_i^{lo}(\mathbf{k}, \omega) = 0, \quad (1.65)$$

where  $\chi_e^{lo}$  and  $\chi_i^{lo}$  are the electron and ion susceptibilities, respectively. For low phase velocity, it follows  $\omega \ll kv_{Fe}$ ,  $\chi_i^{lo}(\mathbf{k}, \omega) = -\Omega_p^2/\omega^2$ , resulting in

$$1 + \frac{\omega_p^2}{k^2 v_F^2 + \hbar^2 k^4 / 4m^2} - \frac{\Omega_p^2}{\omega^2} = 0. \quad (1.66)$$

The result for the dispersion can be written as

$$\omega^2 = \frac{\Omega_p^2}{1 + \mathfrak{K}}, \quad (1.67)$$

where  $\mathfrak{K} = \omega_p^2 / (k^2 v_F^2 - \hbar^2 k^4 / 4m^2)$ . For  $\mathfrak{K} \gg 1$ , (1.67) reduces to

$$\omega \simeq kc_q \left( 1 + \frac{\hbar^2 k^4}{4m^2 \omega_p^2} \right)^{1/2}, \quad (1.68)$$

where  $c_q = (E_F/M)^{1/2}$  is the speed of linear electrostatic ion waves in a quantum plasma (the so-called quantum ion-acoustic wave). Note that the relation (1.68) is for a non-relativistic ideal plasma at  $T = 0$ . In the classical limit,  $\hbar \rightarrow 0$ ,  $E_F \ll E_T$ , Eq. (1.68) corresponds to the dispersion relation of the usual ion-acoustic wave in a thermal plasma.

When using the QHD equations, the momentum equation (1.17) for ions can be written as

$$\left( \frac{\partial}{\partial t} + u_i \frac{\partial}{\partial x} \right) u_i = \frac{q_i E}{M}, \quad (1.69)$$

with  $u_i$ , and  $q_i$  being the ion velocity, and ion charge, respectively. The last two terms in (1.17) are ignored for ions due to smallness of ionic quantum effects. Similarly, the electron inertia can be neglected in the limit  $m/M \ll 1$ . The space charge electric field  $E = -\partial\phi/\partial x$  couples ions with the electrons.

If there exists a drift between electrons and ions in a quantum plasma, the Buneman mode appears [79] just like the classical plasmas [80]. Taking into account collision effects in the electron and ion momentum equations with  $\nu_{en}$  ( $\nu_{in}$ ) being the collision frequencies of an electron (ion) with neutrals<sup>20</sup>, the dispersion relation in the reference frame of the drifting ions becomes

$$1 - \frac{\omega_p^2}{(\omega - kv_0)(\omega - kv_0 + i\nu_{en}) - \hbar^2 k^4 / 4m^2} - \frac{\Omega_p^2}{\omega(\omega + i\nu_{in})} = 0, \quad (1.70)$$

<sup>20</sup> This approximation assumes a weakly ionized plasma where neutrals dominate and, hence, collisions with neutrals play the main role. This is the case at low temperature and not too high densities below the Mott point.

where the relative electron-ion equilibrium drift velocity in the presence of a static electric field  $E_0$  is

$$v_0 = -eE_0 \left( \frac{1}{mv_{en}} + \frac{1}{Mv_{in}} \right). \quad (1.71)$$

For very low frequencies,  $\omega \ll v_{in} \ll kv_0$ ,  $v_{en} \ll kv_0$ , the dispersion equation predicts that the mode is unstable under the condition

$$\omega_p^2 > k^2 v_0^2 - \frac{\hbar^2 k^4}{4m^2} > 0, \quad (1.72)$$

because  $\Im(\omega) > 0$ , otherwise it is damped. The small wavelength oscillations are stable due to the presence of quantum effects. For a slow temporal dynamics, appropriate rescaling of the parameters gives rise to electron momentum equation of the form

$$v_e \frac{\partial v_e}{\partial x} = -E + \frac{F^2}{2} \frac{\partial}{\partial x} \left( \frac{\partial^2 \sqrt{n_e} / \partial x^2}{\sqrt{n_e}} \right), \quad (1.73)$$

provided  $v_{en} \ll \omega_p$  with  $F = \hbar\omega_p/mv_0^2$  being the dimensionless parameter which measures the contribution of quantum potential. The linearization of the normalized set of equations around homogenous equilibrium leads to the dispersion relation with imaginary part of the frequency

$$\omega_i = \frac{k^2 (1 - F^2 k^2 / 4)}{1 - k^2 + F^2 k^4 / 4}, \quad (1.74)$$

where  $\Omega_p \ll v_{in}$ . When the quantum parameter  $F = 0$  (classical limit),  $\omega_i =$

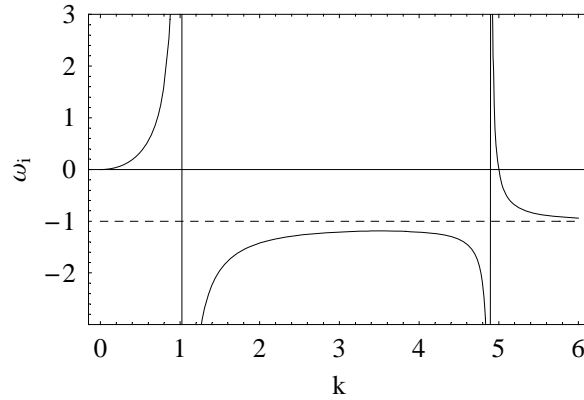


**Fig. 1.5** Instability growth rate from Eq. (1.74) is plotted as a function of normalized wave number  $k$  for  $F = 0.4$ . Two asymptotic values of  $k$  are denoted by  $k_1$  and  $k_2$ . Instability occurs at  $0 < k < k_1$  and  $k_2 < k < k_3$ . The growth rate  $\omega_i \rightarrow -1$  as  $k \rightarrow \infty$ , in both the cases of zero and nonzero  $F$ .

$k^2/(1-k^2)$ . Then, a singularity appears at  $k = 1$  and a linear instability exists for  $0 < k < 1$ . For non-zero  $F$ , various instability conditions emerge for  $F < 1$ ,  $F = 1$ , and  $F > 1$ . We consider one example of the growth rate in the weak coupling regime,  $0 < F < 1$ , as shown in Fig. 1.5, which has two asymptotic values,  $k_1$  and  $k_2$ , given by

$$k_1^2 = \frac{2}{F^2}[1 - \sqrt{1 - F^2}], \quad (1.75)$$

$$k_2^2 = \frac{2}{F^2}[1 + \sqrt{1 - F^2}]. \quad (1.76)$$

The growth rate is positive for  $0 < k < k_1$ , or  $k_2 < k < k_3$ , where

$$k_3^2 = k_1^2 + k_2^2 = \frac{4}{H^2}. \quad (1.77)$$

This case of Buneman instability in collisional quantum plasma is formally similar to the two-stream instability already discussed in Sec. 1.2.6.3 above.

### 1.2.7 Nonlinear waves in quantum plasmas

In the preceding section, we have discussed linearized QHD results following the standard procedure of linearization. When the amplitude of a wave in plasma grows sufficiently large, the nonlinearities in the QHD equations grow and cannot be neglected any more. This makes the system more complicated and its analysis more difficult. The nonlinearities in plasmas may enter through various processes like advection, trapping of particles in the wave potential, the nonlinear Lorentz force, ponderomotive force, etc. Sometimes, the nonlinearities in plasma contribute to the localization of waves giving rise to different types of interesting coherent structures, for instance solitary waves, shocks, vortices, and so on.

Due to highly nontrivial physics involved in the nonlinear regime of quantum plasmas, only a limited analysis has been done in QHD so far. As was shown above the *nonlinear Schrödinger (NLS) equation* (1.28) is equivalent to the QHD in many respects. It has many properties characteristic of nonlinear waves, especially localized modes and solitons, and beam-driven waves and instabilities. The NLS equation and its variants describe nonlinear physical systems appearing in a wide spectrum of problems in (quantum) plasmas<sup>21</sup> and other fields, for example, in fluids and water waves, ultrafast transmission systems, condensed matter systems, and so on. NLS contains an additional nonlinear term in the Schrödinger equation responsible for the nonlinear effects. The solution of NLS Eq. (1.28) also facilitates the verification of numerical solvers and aids in the stability analysis. Discrete nonlinear Schrödinger (DNLS) equations are also important in discrete lattice models in nonlinear optics,

<sup>21</sup> always assuming that the applicability conditions of QHD are fulfilled.



condensed matter and trapped Bose-Einstein condensates where a numerical evaluation is straightforward using e.g. the Crank-Nicolson method, e.g. [81].

The third and fourth terms on the right-hand side of Eq. (1.28) represent the nonlinearities associated with the nonlinear coupling between the electrostatic potential and the quantum statistical pressure associated with Fermi-Dirac statistics. Linearizing the NLS-Poisson system gives the frequency spectrum (1.38) where  $n = |\Psi|^2$ . In equilibrium,  $\tilde{V} \sim n^2 = \text{constant}$ , otherwise it is repulsive because  $\tilde{V}$  is derived from  $p^c(n)$  which is related to the dispersion of velocities in a Fermi gas. The NLS equation admits modulational wave solutions and a stability analysis can be performed by standard procedures. Depending upon the type of nonlinearity, it is also capable to provide valuable information of the quasi-stationary structures and nonlinear interaction mechanisms of waves at various length scales [42].

The fluid modeling of the nonlinear long-wave-short-wave interaction in plasmas is provided by the *Zakharov equations*, first derived by Zakharov [82], which get modified in quantum plasmas [83, 84]. The derivation of the *quantum Zakharov system* follows a two-time scales analysis of the QHD equations which becomes possible due to the presence of fast (Langmuir-type) and slow (ion-acoustic) oscillations. The limitations of the model are similar to QHD and the allowed wavelengths are  $\lambda \gg \lambda_{TF}$ , or, equivalently,  $k\lambda_{TF} \ll 1$ . All QHD variables, i.e., the electron (ion) macroscopic density  $n_e$  ( $n_i$ ), velocity  $u_e$  ( $u_i$ ), and electric field  $E$  are separated into fast (subscript f) and slow (subscript s) oscillatory components

$$n_e(x, t) = n_0 + n_{es}(x, t) + n_{ef}(x, t), \quad (1.78)$$

$$n_i(x, t) = n_0 + n_{is}(x, t), \quad (1.79)$$

$$u_e(x, t) = u_{es}(x, t) + u_{ef}(x, t), \quad (1.80)$$

$$u_i(x, t) = u_{is}(x, t), \quad (1.81)$$

$$E(x, t) = E_s(x, t) + E_f(x, t). \quad (1.82)$$

The slowly varying quantities are considered not significantly changing over a period of oscillation whereas the fast quantities assume zero average. In addition, the quasi-neutrality condition,  $n_e \approx n_i$ ,  $u_e \approx u_i$  is assumed, and the high frequency ion terms are disregarded due to the smallness of  $m/M$ . This analysis is in the spirit of a classical plasma with the inclusion of the quantum (Bohm) potential for a zero-temperature electron (Fermi) gas. In 1D, this gives the quantum corrected Zakharov equations

$$i \frac{\partial E}{\partial t} + \frac{\partial^2 E}{\partial x^2} - H^2 \frac{\partial^4 E}{\partial x^4} = nE, \quad (1.83)$$

$$\frac{\partial^2 n}{\partial t^2} - \frac{\partial^2 n}{\partial x^2} + H^2 \frac{\partial^4 n}{\partial x^4} = \frac{\partial^2 |E|^2}{\partial x^2}, \quad (1.84)$$

where  $E$  and  $n$  are normalized quantities describing the slowly varying envelope field and plasma density, respectively, and quantum corrections are included via the non-dimensional quantum parameter  $H = \hbar\Omega_p/E_{Te}$  with  $\Omega_p$  being the ion plasma frequency and  $E_{Te}$  the electron thermal energy. The system can admit periodic,

chaotic or similar states, and describes nonlinear dynamics and instabilities. The extension of (1.83)-(1.84) to three dimensions makes the inclusion of electromagnetic effects possible [84].

The nonlinear effects causes the distortion of waves in plasma . Then, wave steepening can occur until some dispersive or dissipative process kicks in which broadens the profile, in turn balancing the nonlinear steepening. Haas and co-workers [78] have attempted to include the quantum effects in nonlinear ion wave excitations in the small and large amplitude regimes in the QHD framework. In the small amplitude limit, the 1D QHD equations (1.15), (1.17)-(1.18) and (1.69) reduce through multiscale expansion with appropriate rescaling of parameters to some form of *Korteweg-de Vries (KdV)* equation. Assuming  $m/M \ll 1$ , the electron momentum equation (1.17) with the boundary condition  $n_e = 1$ ,  $\varphi = 0$  at infinity leads to

$$\varphi = -\frac{1}{2} + \frac{n_e^2}{2} - \frac{\Gamma_q}{2} \left[ \frac{\partial_x^2 \sqrt{n_e}}{\sqrt{n_e}} \right], \quad (1.85)$$

where the non-dimensional quantum parameter  $\Gamma_q = (\hbar\omega_p/E_F)^2$ . For  $\Gamma_q = 0$ , the charge density is directly related to the potential by an algebraic equation. We now introduce the slowly varying stretched coordinates

$$\xi = \varepsilon^{1/2}(x-t), \quad \tau = \varepsilon^{3/2}t, \quad (1.86)$$

where  $\varepsilon$  is a small parameter proportional to the amplitude of the perturbation which provides the basis of the scaling, merely a convention. Then, expanding the state variables into a series in powers of  $\varepsilon$ , the low orders of  $\varepsilon$  result in a KdV type equation with quantum corrections given by

$$\frac{\partial \Phi}{\partial \tau} + 2\Phi \frac{\partial \Phi}{\partial \xi} + \frac{1}{2} \left( 1 - \frac{\Gamma_q}{4} \right) \frac{\partial^3 \Phi}{\partial \xi^3} = 0, \quad (1.87)$$

which admits solitary ion wave and periodic solutions. The function  $\Phi(\xi, \tau)$  arises from the zero order solutions and the boundary conditions.

It is important to discuss the features of the dispersive term in Eq. (1.87). The equation is obtained by employing the reductive perturbative technique and the term containing the quantum diffraction (coupling) parameter  $\Gamma_q$  appears from the electron equation (1.85). For  $\Gamma_q = 4$ , the dispersive term in Eq. (1.87) disappears. In this case, the quantum diffraction exactly matches the classical dispersion term in the KdV equation. Then, no soliton solution exists and only free streaming is possible like for a free ideal classical fluid which eventually produces a shock wave. Recall that the parameter  $\Gamma_q$  is related to the coupling strength of the plasma. Since the applicability of QHD (as discussed in Sec. 1.2.5 above) is limited to weak coupling,  $\Gamma_q < 1$  the value  $\Gamma_q = 4$  is certainly out of the scope of QHD. Nevertheless such values are often considered and we present one example below to illustrate the mathematical consequences. For  $\Gamma_q \neq 4$ , setting the wave-frame position variable  $\eta = \xi - V_0\tau$  with constant wave phase velocity  $V_0$  leads to akin to energy first integral for a particle of unit mass in a (pseudo) potential well (Sagdeev-like potential)

whose localized solution depends upon  $\Gamma_q$  and  $V_0$ . A general profile of the potential  $V(\Phi)$ , for different values of  $\Gamma_q$  and  $V_0 > 0$ , is shown in Fig. 1.6 which exhibits the localized (soliton) structure. For  $\Gamma_q < 4$  and  $V_0 > 0$ , some algebra leads to a solitary

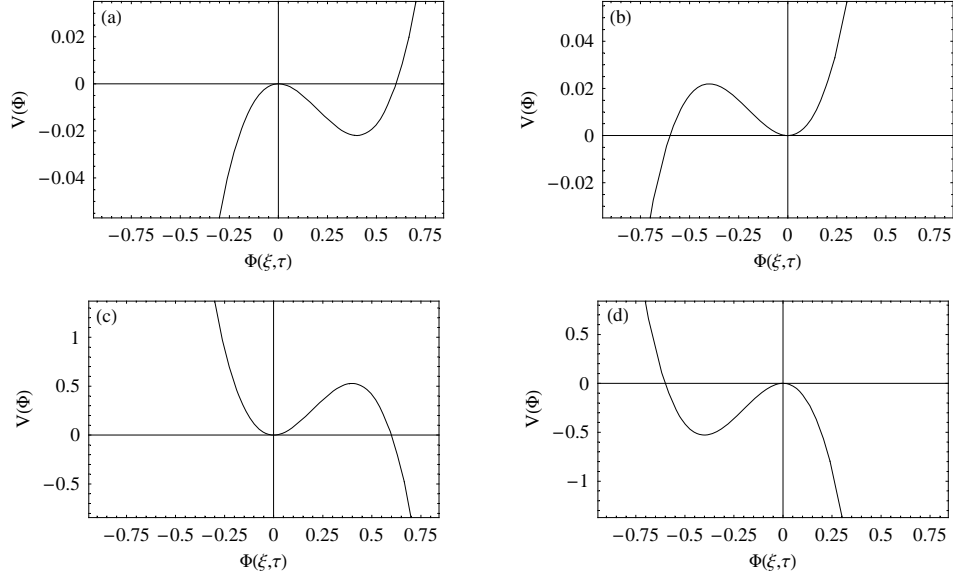


**Fig. 1.6** The potential  $V(\Phi)$  versus  $\Phi(\xi, \tau)$  for arbitrary constant phase velocity  $V_0$  is shown for small and large values of  $\Gamma_q$ . (a):  $\Gamma_q = 0.1$ ,  $V_0 = 0.4$ , (b):  $\Gamma_q = 0.1$ ,  $V_0 = -0.4$ , (c):  $\Gamma_q = 4.1$ ,  $V_0 = 0.4$ , (d):  $\Gamma_q = 4.1$ ,  $V_0 = -0.4$ . The conditions of solution;  $V'(\Phi) = 0$  at  $\Phi = 0$  and  $\Phi = V_0$  are satisfied where prime denotes the derivative with respect to  $\eta$ .

pulse solution of (1.87) of the form

$$\Phi(\xi, \tau) = \frac{3V_0}{2} \operatorname{sech}^2 \left( \frac{\eta}{\sqrt{(4 - \Gamma_q)/2V_0}} \right), \quad (1.88)$$

as shown in Fig. 1.7 as a typical case. The pulse height scales as  $V_0$  whereas the pulse width as  $V_0^{-1/2}$  which also depends upon  $\Gamma_q$ . The larger amplitude pulses are sharper and can propagate with higher speed.

For fully nonlinear large-amplitude localized ion waves, one can define some non-dimensional parameter playing the role of the Mach number. The wave form can be introduced via the variable,

$$\xi = (x - Mt), \quad (1.89)$$

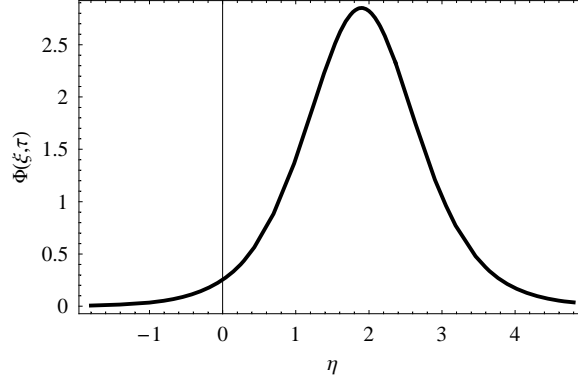


**Fig. 1.7** The solitary pulse profile for  $\Gamma_q = 0.1$  and arbitrary constant phase velocity  $V_0 > 0$ . For such small values of  $\Gamma_q$ , the effect on pulse width is negligibly small.

with  $M$  being the Mach number. Then, the QHD equations reduce to the dynamical equations which can be written in the form of conservation laws leading to solitary wave solutions depending upon  $\Gamma_q$  and  $M$ .

### 1.2.8 Magnetized quantum plasmas

So far, we have considered only the electrostatic case. The inclusion of a magnetic field leads to a more general form of the QHD equations derivable from the electromagnetic Wigner equation. Following the procedure similar to the unmagnetized plasma case, the Madelung decomposition of the ensemble wave functions allows to identify the classical and quantum parts of the pressure dyad. Considering the statistical mixture of  $K$ – states  $\psi_i = \psi_i(\mathbf{r}, t)$ ,  $i = 1, \dots, K$ , such that the probabilities  $p_i \geq 0$ , with  $\sum_{i=1}^K p_i = 1$ , each  $\psi_i$  obey the Schrödinger equation

$$i\hbar \frac{\partial \psi_i}{\partial t} = \frac{1}{2m} (-i\hbar \nabla - q\mathbf{A})^2 \psi_i + q\varphi \psi_i, \quad (1.90)$$

where the charge carriers have mass  $m$  and charge  $q$  under the influence of self-consistent scalar and vector potentials  $\varphi(\mathbf{r}, t)$  and  $\mathbf{A}(\mathbf{r}, t)$ , respectively, with choice of Coulomb gauge  $\nabla \cdot \mathbf{A} = 0$ . Then the one-particle Wigner function in terms of coordinate  $\mathbf{r}$  and momentum  $\mathbf{p} = m\mathbf{v} + q\mathbf{A}$  becomes

$$f_W(\mathbf{r}, \mathbf{p}, t) = \frac{1}{(2\pi\hbar)^3} \sum_{i=1}^K p_i \int_{-\infty}^{\infty} d\mathbf{s} \psi_i^* \left( \mathbf{r} + \frac{\mathbf{s}}{2}, t \right) e^{i\mathbf{p} \cdot \mathbf{s} / \hbar} \psi_i \left( \mathbf{r} - \frac{\mathbf{s}}{2}, t \right), \quad (1.91)$$

which leads to the evolution equation for  $f_W$  – the quantum Vlasov equation – obtained after a cumbersome calculation, for details, see [49]. Since, the complexity of the Wigner function equation in the electrostatic case makes it very hard to be fully examined, except for the simpler linear case. For a non-zero magnetic field, the problem becomes even more challenging and the analysis more difficult which motivates hydrodynamic description.

Introducing the moment equations in the usual way, the continuity and the momentum transport equations in a magnetized plasma following from the Wigner function equation can be written as

$$\frac{\partial n}{\partial t} + \frac{\partial (n\mathbf{u})}{\partial x} = 0, \quad (1.92)$$

$$\frac{\partial \mathbf{u}}{\partial t} + \mathbf{u} \cdot \nabla \mathbf{u} = \frac{q}{m} (\mathbf{E} + \mathbf{u} \times \mathbf{B}) - \frac{1}{mn} \nabla p^c(n) + \frac{\hbar^2}{2m^2} \nabla \left( \frac{\nabla^2 \sqrt{n}}{\sqrt{n}} \right), \quad (1.93)$$

where the closure assumption is made by defining a diagonal form of the classical pressure dyad. Since the classical part of the pressure dyad  $p^c$  can be written as the sum of average velocity dispersions, the diagonal isotropic form assumes the components

$$P_{ij} = \delta_{ij} p^c, \quad (1.94)$$

with  $p^c = p^c(n)$  being a suitable equation of state. For  $\hbar \rightarrow 0$ , (1.93) is just like the momentum equation of classical fluids. Equations (1.92)-(1.93) together with Maxwell's equations constitute the QHD model for magnetized plasmas where the limitations of the electrostatic QHD equations are also valid in the present case. For more subtle issues like gauge invariance of Wigner equation, magnetohydrodynamic equilibria, the inclusion of spin and strong field effects (Landau quantization) etc., see [49].

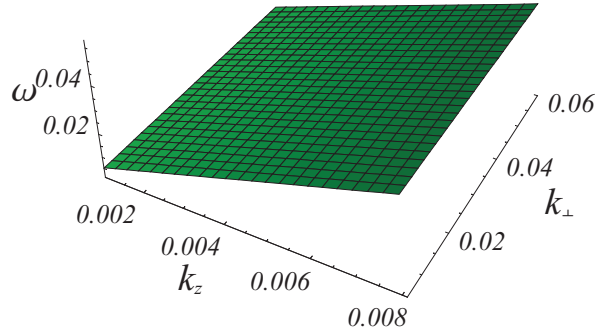


**Fig. 1.8** Low-frequency electromagnetic mode in a strongly degenerate electron plasma with immobile ions. The wave frequency is normalized by  $\omega_c$  and the wave numbers by  $v_F/\omega_c$ .

### 1.2.8.1 Electrostatic and electromagnetic low frequency modes

We start from the QHD equations for a two-component dense uniform magnetized plasma consisting of degenerate electrons and non-degenerate ions. Assuming the dynamics of electrons with a background of stationary ions embedded in a uniform magnetic field  $B_0 \hat{\mathbf{z}}$ , the low-frequency (in comparison with the electron cyclotron frequency) electric and magnetic field perturbations are defined as  $\mathbf{E} = -\nabla\phi - c^{-1}(\partial A_z/\partial t)\hat{\mathbf{z}}$  and  $\mathbf{B}_\perp = \nabla_\perp A_z \times \hat{\mathbf{z}}$ , respectively. From (1.93), assuming low frequencies,  $\omega \sim |\partial/\partial t| \ll \omega_c, ck$ , but  $\omega$  higher than the ion plasma frequency  $\Omega_p$ , and ion cyclotron frequency,  $\Omega_c$ , respectively, the linearized components of the electron and ion fluid velocity parallel and perpendicular to  $\hat{\mathbf{z}}$  become

$$\frac{\partial v_{jz}}{\partial t} = \delta_j \frac{e}{m} \left( \frac{\partial \phi_j}{\partial z} + \frac{1}{c} \frac{\partial A_z}{\partial t} \right), \quad (1.95)$$

$$\mathbf{v}_{j\perp} \simeq \frac{c}{B_0} \left( \hat{\mathbf{z}} \times \nabla_\perp \phi_j + \delta_j \frac{1}{\omega_c} \frac{\partial \nabla_\perp \phi_j}{\partial t} \right), \quad (1.96)$$

where  $j = e(i)$  denotes electron (ion),  $\delta_e = 1$ ,  $\delta_p = -1$ , and we denoted  $\phi_j = \phi - \frac{\delta_j}{n_0 e} \left( \frac{2E_F}{3} - \frac{\hbar^2 \nabla^2}{4m} \right) n_j$ , with  $n_j \ll n_0$ . The dispersion relation for the shear electromagnetic mode in this case is derived by employing (1.95)-(1.96), together with the linearized continuity equation, Poisson's equation and Ampere's law which, upon Fourier transformation, results in

$$\omega^2 = \frac{c^2 k_z^2 k_\perp^2 (1 + \Lambda_q^2 k^2)}{(1 + \lambda_e^2 k_\perp^2) \left[ k^2 + k_\perp^2 (1 + \Lambda_q^2 k^2) \frac{\omega_p^2}{\omega_c^2} \right]}, \quad (1.97)$$

which shows the influence of the electron quantum statistical and quantum diffraction effects [Fig. 1.8], where  $\lambda_e = c/\omega_p$ ,  $\Lambda_q = v_q/\omega_p$ , and  $v_q = \sqrt{T_q/m}$  with  $T_q = (\hbar^2 k^2/4m + 2E_F/3)$  being the quantum parameter in energy units playing the same role as effective temperature in classical plasmas [85]. The electromagnetic mode (1.97) ceases to exist for  $k_z = 0$ .

Next, we consider the ion dynamics in the frequency regime  $\omega \ll \Omega_c$ . The ion perpendicular velocity component then consists of the electric and ion polarization drifts,  $\mathbf{v}_E$  and  $\mathbf{v}_p$  respectively. Then the dispersion equation with assumption of  $k_z \ll k_\perp$  acquires the form

$$\left[ (1 + K_A^2) \omega^2 - \frac{c_q^2 k_z^2}{(1 + \lambda_e^2 k_\perp^2)} (1 + K_A^2) \right] \omega^2 - \frac{\omega_A^2}{(1 + \lambda_e^2 k_\perp^2)} \left[ \left( 1 + \frac{c_q^2 k^2}{\omega_{pi}^2} \right) \omega^2 - c_q^2 k_z^2 \right] = \frac{\rho_q^2 k_\perp^2 \omega_A^2}{(1 + \lambda_e^2 k_\perp^2)} \omega^2, \quad (1.98)$$

where  $K_A = \frac{v_A}{ck_\perp/k}$ ,  $v_A = B_0/\sqrt{4\pi n_0 M}$  is the speed of the Alfvén wave,  $c_q = \sqrt{T_q/M}$  is the speed of the electrostatic ion wave, and  $\rho_q = c_q/\Omega_c$ . The co-existing electro-

static and electromagnetic modes [Fig. 1.9] are well separated, however, the difference of frequencies become lesser and lesser as the magnetic field is increased. In

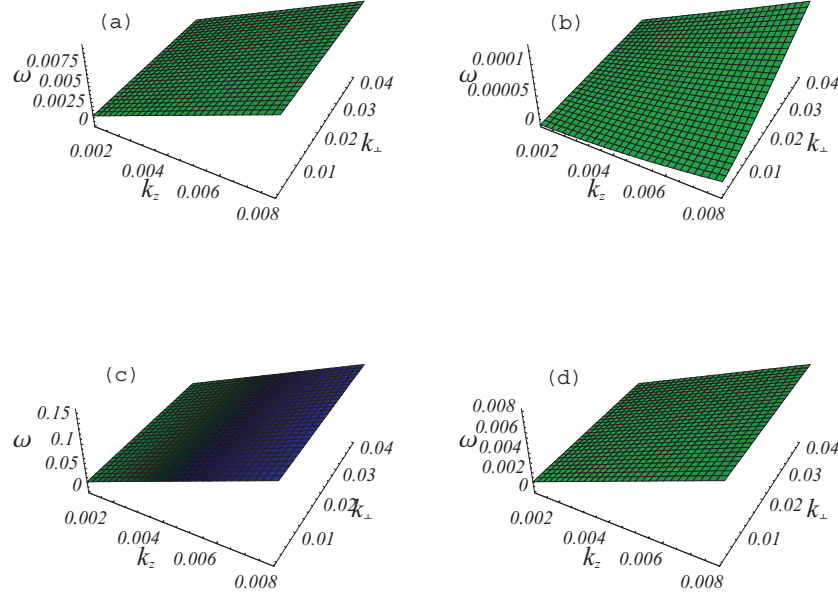


**Fig. 1.9** Low-frequency linear electrostatic (a,c) and electromagnetic (b,d) modes in a magnetized quantum plasma in the absence (upper panel) and the presence (lower panel) of degeneracy pressure for typical quantum plasma of white dwarf stars taken from Table 1.2 with density  $\sim 10^{26} \text{cm}^{-3}$  and magnetic field  $\sim 10^8 \text{G}$ . The dispersion relation shows that the electrostatic (quantum ion-acoustic) mode can couple with the electromagnetic (shear Alfvén) mode in high magnetic field regions where the difference of frequencies become small. The wave frequency is normalized by  $\Omega_c$  and wave numbers by  $v_A/\Omega_c$ .

the limiting case, for  $v_A \ll ck_\perp/k$ ,  $\lambda_e^2 k_\perp^2 \ll 1$ , (1.98) reduces to

$$\omega^2 = k_z^2 v_A^2 (1 + \rho_q^2 k_\perp^2), \quad (1.99)$$

which shows the dispersive Alfvén wave where the dispersion comes from the electron quantum effects.

### 1.2.8.2 Drift mode

In the presence of gradients (inhomogeneities in density, temperature, etc.), there may appear drift waves in classical as well as quantum plasmas which play an important role in transport of plasma particles and energy/momentum across the magnetic field lines. Drift waves are low frequency waves in comparison with the ion cyclotron frequency  $\Omega_c$  with perpendicular (with respect to the magnetic field)

wave number  $k_{\perp}$  much larger than  $k_{\parallel}$ . For relatively large  $k_{\parallel}$ , the drift wave can couple with the quantum ion acoustic wave [86]. Consider a dense quantum plasma embedded in a constant external magnetic field in z-direction possessing a density inhomogeneity at equilibrium in the x-direction such that  $\nabla n_{j0} = -(\frac{dn_{j0}}{dx})\hat{\mathbf{x}}$ , and  $\kappa_{jn} = |\frac{1}{n_{j0}} \frac{dn_{j0}}{dx}| = \text{constant}$ , with  $\kappa_{jn} \ll k_{\perp}$ . Using the QHD equations with the electric and magnetic field perturbations as given in the previous section, the dispersion relation for drift waves in quantum plasma becomes

$$\left[ (\omega - \omega_q^*)\omega - \frac{c_q^2 k_z^2}{(1 + \lambda_e^2 k_{\perp}^2)} \right] \omega^2 - \frac{\omega_A^2}{(1 + \lambda_e^2 k_{\perp}^2)} [\omega^2 - \omega_q^* \omega - c_q^2 k_z^2] = \frac{\rho_q^2 k_{\perp}^2 \omega_A^2}{(1 + \lambda_e^2 k_{\perp}^2)} \omega^2, \quad (1.100)$$

where  $\omega_A = k_z v_A$  is the frequency of the Alfvén wave,  $\omega_q^* = \mathbf{v}_{qD} \cdot \mathbf{k}$  is the drift wave frequency,  $\mathbf{v}_{qD} = \frac{c T_q}{e B_0} \nabla \ln n_0 \times \hat{\mathbf{z}}$  is the drift wave velocity, and  $T_q = \hbar^2 k^2 / 4m$ . The

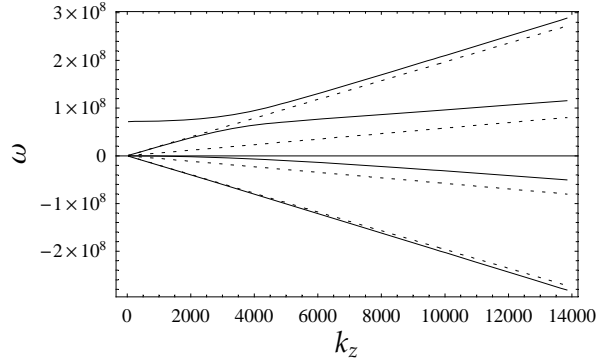


**Fig. 1.10** The appearance of a drift mode in a magnetized non-uniform quantum plasma due to density inhomogeneity. The frequencies of the four low-frequency modes (in units of  $s^{-1}$ ) are plotted vs. the wave numbers  $k_z$  for fixed  $k_y$  (units of  $cm^{-1}$ ) for a dense astrophysical plasma with typical parameters selected from Table 1.2 with density  $\sim 10^{27} cm^{-3}$  and magnetic field  $\sim 10^6 G$ . One branch of the shear Alfvén wave and one branch of the electrostatic wave are influenced by the quantum drift wave  $\omega_q^*$  near  $k_z \sim 4 \times 10^3 cm^{-1}$ . The dashed lines represent  $\pm k_z v_A$  (outer lines) and  $\pm k_z c_q$  (inner lines), respectively. From Ref. [86].

above relation has an analogy with the classical drift wave frequency which depends upon the equilibrium electron pressure defined by the ideal gas law. However, both are very different physically. The classical drift wave depends upon electron thermal energy, but in a quantum plasma, the role of thermal energy is taken over by the Fermi energy. In deriving (1.100), the drift approximation  $|\partial_t| \ll \Omega_c$  is used in the limit of small Fermi pressure. In Fig. 1.10, the frequencies of the four modes are plotted against  $k_z$ . One branch of the shear Alfvén wave and one branch of the elec-



trostatic wave are influenced by the quantum drift wave  $\omega_q^*$  near  $k_z \sim 4 \times 10^3 \text{ cm}^{-1}$ . Since  $T_i = 0$  has been assumed, therefore the second branch of the Alfvén wave remains a straight line in this figure. The second branch of the electrostatic wave has also the effects of dispersion similar to the classical case. The density matrix approach can also be used to study quantum drift wave in two component inhomogeneous plasma in a strong magnetic field under strong and weak quantum effects [87]. Here, the problem is treated semiclassically with a modified Maxwell distribution function in order to determine the quantum effects. Such waves become unstable under some circumstances.

Concluding this section, let us briefly discuss for what systems the present results can be relevant. In the QHD approach, the effect of Fermi degeneracy and (quantum) Bohm potential are the main quantum ingredients. The applications of nonlinear waves with or without magnetic field can be found in dense quasi-free electron gas and in the high density regimes relevant to degenerate plasmas of dense astrophysical objects (regions of white dwarfs and neutron stars). Such densities are also expected in the lab in next generation laser-plasma experiments. At such high densities,  $r_s$  will be well below unity and the QHD model may be even better applicable.

Let us consider a typical example from Table 1.2, with density  $n_0 = 4.0 \times 10^{26} \text{ cm}^{-3}$ ,  $\bar{r} = 8.3 \times 10^{-10} \text{ cm}$  and  $\lambda_{TF} = 7.2 \times 10^{-8} \text{ cm}$ . The wave number  $k$  should be well below  $\bar{r}^{-1}$  for both electronic and ionic perturbations. For low frequency perturbations, if  $k \simeq 10^6 \text{ cm}^{-1}$ , the ion wave speed is  $c_q \simeq 3.8 \times 10^7 \text{ ms}^{-1}$  and the frequency, from Eq. (1.66) is  $\simeq 6 \times 10^{13} \text{ s}^{-1}$ . If we consider the soliton solution, Eq. (1.88), for such a plasma, the effect of the quantum parameter  $\Gamma_q$  is vanishingly small since  $\Gamma_q \leq 1$  for applicability of the QHD approximation. Due to the very high density, the inter-particle distances are very small. In the weakly nonlinear limit, a soliton with a typical speed  $\sim 0.1c_q$  shows very small amplitude and width parameters. For a magnetized plasma with high ambient magnetic field ( $B_0 \simeq 1 \times 10^7 \text{ G}$ ) and low frequency electrostatic and electromagnetic perturbations, dispersion equation Eq. (1.98) with  $k_z/k_\perp \simeq 0.002$  reveals that the frequency of electrostatic mode is  $1.4 \times 10^{13} \text{ s}^{-1}$ . Similarly, the frequency of the shear Alfvén mode is  $3.1 \times 10^9 \text{ s}^{-1}$ , with  $v_A = 2.2 \times 10^5 \text{ ms}^{-1}$  being the speed of the wave. It should be noted that the modes are well separated for low magnetic field but their frequencies get closer and closer as the magnetic field increases.

### 1.3 Interaction and spin effects in Quantum Plasmas

As was discussed above, QHD assumes an (almost) ideal electron Fermi gas. There have recently been attempts to include exchange and correlation effects in order to extend the validity range of QHD which we briefly discuss below.

The first attempt to include exchange and correlation effects in QHD phenomenologically was presented by Manfredi and co-workers in Ref. [48]. Inspired by

the procedure used in density functional theory (DFT) they used an additional exchange-correlation functional,  $V_{xc}$

$$V_{xc} = 0.985(e^2/\varepsilon)n^{1/3}[1 + (0.034/a_B n^{1/3})\ln(1 + 18.37a_B n^{1/3})], \quad (1.101)$$

in the momentum equation that gives rise to an additional force on the electrons. The authors performed comparisons with DFT simulations for electrons in condensed matter and observed reasonable agreement.

### 1.3.1 Prediction of attractive forces between protons in quantum plasmas

Using the QHD with the above mentioned potential  $V_{xc}$  Shukla and Eliasson [88] considered the problem of the effective potential of a proton embedded in a dense quantum plasma. The QHD equations together with the Poisson's equation for the electrostatic potential are

$$\begin{aligned} \frac{\partial n}{\partial t} + \nabla \cdot (n\mathbf{u}) &= 0, \\ m_* \left( \frac{\partial \mathbf{u}}{\partial t} + \mathbf{u} \cdot \nabla \mathbf{u} \right) &= e\nabla\phi - n^{-1}\nabla P + \nabla V_{xc} + \nabla V_B, \end{aligned} \quad (1.102)$$

$$\nabla^2 \phi = \frac{4\pi e}{\varepsilon}(n - n_0) - 4\pi Q\delta(\mathbf{r}), \quad (1.103)$$

where the positive test charge  $Q$  is located at  $\mathbf{r} = 0$ . Quantum effects are taken into account as usual via the Bohm potential  $V_B = (\hbar^2/2m_*)(1/\sqrt{n})\nabla^2\sqrt{n}$ . The pressure of the ideal Fermi gas at zero temperature,  $P = (n_0 m_* v_*^2/5)(n/n_0)^{5/3}$ , is used and complemented by the exchange-correlation potential  $V_{xc}$ . Here, the following definitions are used:  $\varepsilon$  denotes the relative dielectric permeability of the material,  $v_* = \hbar(3\pi^2)^{1/3}/m_* r_0$  is the electron Fermi speed,  $r_0 = n_0^{-1/3}$  is the Wigner-Seitz radius, and  $m_*$  is the effective mass of electron.

Shukla and Eliasson linearized these equations, writing  $n = n_0 + n_1$  and  $|n_1| \ll n_0$ . Neglecting dynamic effects in the dielectric function,  $\varepsilon(\mathbf{k}, \omega) = \varepsilon(\mathbf{k}, 0)$ , the electrostatic potential of a proton is given by

$$\phi(\mathbf{r}) = \frac{Q}{2\pi^2} \int \frac{\exp(i\mathbf{k} \cdot \mathbf{r})}{k^2 \varepsilon(\mathbf{k})} d^3 k. \quad (1.104)$$

From the linearized QHD equations they obtained for the inverse dielectric function

---

<sup>21</sup> The effective mass takes into account medium effects for the case of electrons in condensed matter systems. Here we will focus on electrons in a hydrogen plasma where  $m_*$  coincides with the free electron mass.

$$\frac{1}{\varepsilon(k)} = \frac{(k^2/k_s^2) + \alpha k^4/k_s^4}{1 + (k^2/k_s^2) + \alpha k^4/k_s^4}, \quad (1.105)$$

with the definitions

$$\alpha = \hbar^2 \omega_{pe}^2 / 4m_*^2 (v_*^2/3 + v_{ex}^2)^2, \quad (1.106)$$

$$k_s = \omega_{pe} / \sqrt{v_*^2/3 + v_{ex}^2}, \quad b_* = 1/\sqrt{4\alpha - 1}, \quad (1.107)$$

$$v_{ex} = (0.328e^2/m_*\varepsilon r_0)^{1/2} [1 + 0.62/(1 + 18.36a_B n_0^{1/3})]^{1/2}, \quad (1.108)$$

$$k_r = (k_s/\sqrt{4\alpha})(\sqrt{4\alpha} + 1)^{1/2}, \quad k_i = (k_s/\sqrt{4\alpha})(\sqrt{4\alpha} - 1)^{1/2}. \quad (1.109)$$

The parameter  $\alpha$  is shown in Fig. 1.11. While for  $\alpha < 0.25$  the potential (1.104)

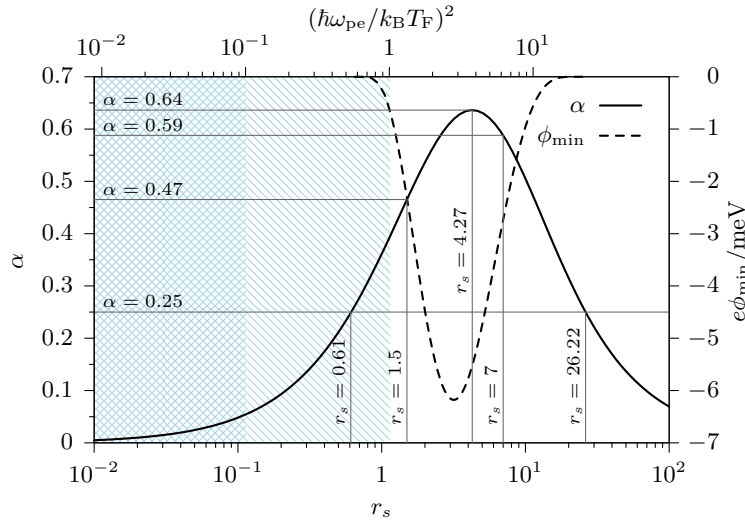


**Fig. 1.11** The Shukla-Eliasson parameter  $\alpha$  (left axis) versus quantum coupling parameters: the Brueckner parameter  $r_s$  (bottom axis) and  $\Gamma_q$  (upper axis). The potential of a proton, Eq. (1.104), derived by Shukla and Eliasson from linearized QHD becomes attractive for  $\alpha > 0.25$ , corresponding to  $26.22 \geq r_s \geq 0.61$ , at zero temperature. The two shaded areas denotes the range of moderate (weak) coupling given by  $(\hbar\omega_{pe}/k_B T_F)^2 < 1$  ( $< 0.1$ ). Also shown is the depth of the SE potential (right axis). From Ref. [91].

is always positive, for  $\alpha > 0.25$ , it develops a negative (attractive) minimum. In the latter case the potential is given by [88]

$$\phi(\mathbf{r}) = \frac{Q}{r} [\cos(k_i r) + b_* \sin(k_i r)] e^{-k_r r}. \quad (1.110)$$

The maximum value of  $\alpha$  is approximately 0.64. Inserting all parameters in the definition of  $\alpha$ , existence of a negative potential in the linearized QHD is confined to a finite density interval where  $0.61 \leq r_s \leq 26.22$ , see Fig. 1.11. Here the standard quantum coupling (Brueckner) parameter has been used,  $r_s = \bar{r}/a_B$ , where  $\bar{r}$  denotes the mean inter-particle distance and  $a_B$  the Bohr radius. For weak coupling,  $r_s \ll 1$ , linearized QHD does not predict a negative potential.

In Ref. [88], based on the existence of a negative minimum of the proton potential (1.104), Shukla and Eliasson claimed the discovery of a novel attractive force between ions in dense quantum plasmas. They claimed that this potential would lead to novel bound states and to a proton lattice. However, as can be seen in Fig. 1.11 where we also show the depth of this potential, negative values occur only in the regime of moderate coupling, i.e. way outside the validity range of QHD which was discussed in Sec. 1.2.5 above. We note that the linearized version of QHD, obviously, is even less accurate. To verify these strong claims, Ref. [70] reported ab initio density functional theory simulations. The DFT result for the effective potential of a proton in dense hydrogen, indeed, was found to exhibit an attractive minimum, in two cases: first, at low density,  $r_s > 1.5$  there is a minimum corresponding to binding of two hydrogen atoms into a molecule. Second, at large distances, there are shallow oscillations of the potential which are related to Friedel oscillations (originating from the step character of the zero-temperature Fermi distribution). No other cases of attractive potentials between protons were observed in the simulations. Therefore, Ref. [70] had to conclude that the predictions of Ref. [88] are wrong.

The disagreement between linearized QHD and DFT was further discussed in Refs. [89, 90]. A careful analysis of the applicability range of QHD and DFT shows that, from its construction, DFT is always more accurate. The lesson to learn from this is that the applicability limits of QHD should be taken very seriously and clearly checked in any application.

### 1.3.2 Spin effects in quantum plasmas

In recent years attempts have been made to extend the QHD to quantum plasmas with spin effects. This is natural as spin effects are always present for quantum particles. For the case of plasmas with degenerate electrons, the effect of fermionic statistics (spin 1/2) has to be considered. The corresponding extension of QHD to spin QHD (SQHD) can be found e.g. in refs. [92, 93, 94] and references therein. These papers came to the conclusion that collective spin effects can dominate the plasma dynamics which is derived from a (possibly macroscopically large) spin magnetization current

$$\mathbf{j}_{\text{spin}} = \nabla \times 2n\mu_B \mathbf{S}, \quad (1.111)$$

where  $n$  is the total electron density,  $\mu_B$  the Bohr magneton and  $\mathbf{S}$  the local average ‘‘spin vector’’. For a high density, as is often the case in quantum plasmas and, as-

suming spin polarization (i.e. all spins are aligned), this current and the associated magnetization may become very large.

It has recently been pointed out [95] that this prediction is in striking contrast to standard condensed matter physics and experiments as well. In particular, the quantum theory of magnetism, e.g. [96, 97, 98] is well developed and does not predict any such gigantic magnetizations. There it is known that the magnetization arises from unpaired electron spins and is proportional to the density of spin up minus spin down electrons,  $n_+ - n_-$ . However, due to Pauli blocking, at low temperature this difference vanishes, it is zero for an ideal Fermi gas in the ground state. At finite temperature, a finite difference may exist which scales as [95]

$$\frac{n_+ - n_-}{n} = O\left(\frac{T}{T_F}\right), \quad (1.112)$$

i.e. in the magnetization not all electrons but only those in a small layer (of order  $T$ ) around the Fermi edge participate resulting in the known moderate values for the spin magnetization of real materials. Thus, at low temperatures when the system approaches an ideal Fermi gas the spin magnetization vanishes, whereas at high temperatures it vanishes as well because all quantum effects are washed out by thermal fluctuations leading to random spin orientations.

The striking contrast between the SQHD prediction, Eq. (1.111) and Eq. (1.112) is surprising since the theoretical concepts that are used in condensed matter physics include correlations and spin effects in a much more accurate fashion than QHD. As is pointed out in the analysis of Ref. [95] the SQHD analysis contains a major inconsistency (see our discussion above): the  $N$ -particle wave function is represented by a product of single-particle orbitals (Hartree or Vlasov approximation) whereas for fermions an anti-symmetrized ansatz has to be used. This leads to Slater determinants that guarantee the Pauli principle, in contrast to the Hartree ansatz. As a result the Fermi statistics and the Pauli principle are lost in key places of the QHD theory. In particular, kinetic effects such as the sharp Fermi surface are lost<sup>22</sup>.

Therefore, the predictions of exotic spin quantum effects in quantum plasmas such as spin-gradient-driven light amplification [94] have to be questioned. While there is always room for new fascinating discoveries they, obviously, have to be based on a well established theory that includes all relevant effects. An urgent next step, to resolve these conflicting predictions is, therefore, to reformulate QHD fully using anti-symmetric  $N$ -particle states, thus building in the Pauli principle from the very beginning.

---

<sup>22</sup> The Fermi distribution is only included via the equation of state relating pressure and density, but this introduces degeneracy effects only in an average fashion.

## 1.4 Conclusion and Outlook

In this chapter, we have discussed the theoretical treatment of dense quantum plasmas that are increasingly important in many laboratory and astrophysical systems. While accurate approaches to quantum plasmas have been in existence for many years – based on first-principle simulation, quantum kinetic theory and non-equilibrium Greens functions – these approaches are quite difficult, especially for magnetized plasmas. This makes it highly desirable to have at hand simpler models. Here quantum hydrodynamics has become quite popular in various scientific areas, as is evident from the vast literature that appeared in recent years. At the same time, most papers have essentially ignored the limited applicability range of QHD raising questions about the reliability of the results and of their relevance for practical applications.

In this chapter, we have discussed the main concepts of quantum hydrodynamics and its relations to quantum kinetic theory in terms of the Wigner distribution function and its equation of motion. We analyzed in detail the basic assumptions that lead to the QHD equations and their limitations. Strictly speaking, QHD applies to an ideal Fermi gas (where the quantum coupling parameters are small, i.e.  $r_s \ll 1$  and  $\Gamma_q \ll 1$ ) at zero temperature, and it entirely neglects quantum exchange effects. Furthermore, as any hydrodynamic theory, QHD is only able to resolve processes at sufficiently large length scales exceeding a threshold which is on the order of the Thomas-Fermi screening length  $\lambda_{TF}$ . Furthermore, QHD uses a closure of the system of hydrodynamic equations that involves an equation of state in the local approximation which again rules out strong inhomogeneities. When any of these inherent limitations is neglected, unphysical results can follow which includes the predictions of attractive forces between protons at atomic scales as well as giant magnetizations related to the electron spin.

In the linearized QHD, we have briefly reviewed some properties of electron and ion plasma oscillations for unmagnetized as well as magnetized quantum plasma. These include the linear electron plasma waves in the strong degeneracy limit at  $T = 0$  as well as for finite  $T$  and their dispersion. This was compared with the results from kinetic theory which also provide information on the damping of the oscillations. We further considered the quantum streaming and Buneman instabilities, and low frequency electrostatic and electromagnetic ion modes in uniform and nonuniform quantum plasma. Finally, an overview of the nonlinear solutions of the QHD equations was given, leading to localized coherent structures and the model equations for a magnetized plasma have been presented with illustrations for the sake of generality.

**Acknowledgements** The authors thank Tim Schoof for valuable remarks. This work has been supported by the Deutsche Forschungsgemeinschaft via SFB-TR24.

## References

1. M. Bonitz, N. Horing, P. Ludwig (eds.), *Introduction to Complex Plasmas* (Springer, Berlin, 2010) Chs. 3 & 4
2. S.A. Maier, *Plasmonics-Fundamentals and Applications* (Springer, New York, 2007)
3. H.A. Atwater, A. Polman, Plasmonics for improved photovoltaic devices, *Nature Mat.* **9**, 205 (2010) and references therein
4. M. Bonitz, R. Binder, S.W. Koch, Carrier-acoustic plasmons instability in semiconductor quantum wires, *Phys. Rev. Lett.* **70**, 3788 (1993)
5. M. Bonitz, R. Binder, D.C. Scott, S.W. Koch, D. Kremp, Theory of plasmons in quasi-one-dimensional degenerate plasmas, *Phys. Rev. E* **49**, 5535 (1994)
6. S.H. Glenzer, R. Redmer, X-ray Thomson scattering in high energy density plasmas, *Rev. Mod. Phys.* **81**, 1625 (2009)
7. C.P. Ridgers, et al., Dense Electron-Positron Plasmas and Ultraintense  $\gamma$ -rays from Laser-Irradiated Solids, *Phys. Rev. Lett.* **108**, 165006 (2012)
8. G. Chabrier, D. Saumon, A.Y. Potekhin, Dense plasmas in astrophysics: from giant planets to neutron stars, *J. Phys. A: Math. Gen.* **39** 4411 (2006)
9. M.H. Thoma, Strongly coupled plasma in high energy physics, *IEEE Trans. Plasma Sci.* **32**, 738 (2004)
10. V.I. Tatarskii, The Wigner representation of quantum mechanics, *Sov. Phys. Usp.* **26**, 311 (1983) [*Usp. Fis. Nauk.* **139**, 587 (1983)]
11. D. Bohm, D. Pines, A Collective Description of Electron Interactions: III. Coulomb Interactions in a Degenerate Electron Gas, *Phys. Rev.* **92**, 609 (1953)
12. Yu.L. Klimontovich, and V.P. Silin, On the spectra of systems of interacting particles, (in Russian) *Zh. Eksp. Teor. Fiz.* **23**, 151 (1952)
13. Yu.L. Klimontovich, V.P. Silin, The spectra of systems of interacting particles, In: *Plasma Physics* ed. by J. Drummond (McGraw-Hill, New York 1961)
14. D. Pines, A Collective Description of Electron Interactions: IV. Electron Interaction in Metals. *Phys. Rev.* **92**, 626 (1953)
15. D. Pines, *Quantum Plasma Physics: Classical and Quantum Plasmas.* *J. Nucl. Energy, Part C* **2**, 5 (1961)
16. P. Nozières, D. Pines, *The Theory of Quantum Liquids* (Benjamin, New York, 1966)
17. G.D. Mahan, *Many-Particle Physics* 2nd edn. (Plenum, New York, 1990)
18. M. Bonitz, D. Semkat (eds.), *Introduction to Computational Methods for Many-Body Physics* (Rinton, Princeton, 2006)
19. V.S. Filinov et al., Monte Carlo simulations of dense quantum plasmas, *J. Phys. A: Math. Gen.* **39**, 4421 (2006)
20. V.S. Filinov, M. Bonitz, A. Filinov, V.O. Golubnychiy, Wigner Function Quantum Molecular Dynamics, In: *Computational Many-Particle Physics, Lec. Notes in Phys. 739*, ed. by H. Fehske, R. Schneider, A. Weiße (Springer, Berlin, 2008)
21. M. Bonitz, A. Filinov, V.O. Golubnychiy, Th. Bornath, W.D. Kraeft, First Principle Thermodynamic and Dynamic Simulations for Dense Quantum Plasmas, *Contrib. Plasma Phys.* **45**, 450 (2005)
22. P. Hohenberg, W. Kohn, Inhomogeneous Electron Gas, *Phys. Rev.* **136**, B864 (1964)
23. W. Kohn, L.J. Sham, Self-Consistent Equations Including Exchange and Correlation Effects, *Phys. Rev.* **140**, A1133 (1965)
24. M.W.C. Dharma-wardana, The Classical-Map Hyper-Netted-Chain (CHNC) Method and Associated Novel Density-Functional Techniques for Warm Dense Matter, *Int. J. Quantum Chemistry* **112**, 53 (2012)
25. F. Perrot, M.W.C. Dharma-wardana, Spin-polarized electron liquid at arbitrary temperatures: Exchange-correlation energies, electron-distribution functions, and the static response functions, *Phys. Rev. B* **62**, 16536 (2000)
26. J.W. Dufty, S. Dutta, Classical representation of a quantum system at equilibrium: Theory, *Phys. Rev. E* **87**, 032101 (2013)

27. S. Dutta, J.W. Dufty, Classical representation of a quantum system at equilibrium: Applications, *Phys. Rev. E* **87**, 032102 (2013)
28. S. Dutta, J.W. Dufty, Uniform electron gas at warm, dense matter conditions, *Eur. Phys. Lett.* **102**, 67005 (2013)
29. M. Bonitz, *Quantum Kinetic Theory* (Teubner, Stuttgart, 1998)
30. D. Kremp, Th. Bornath, M. Bonitz, M. Schlanges, Quantum kinetic theory of plasmas in strong laser fields, *Phys. Rev. E* **60**, 4725 (1999)
31. M. Bonitz, Th. Bornath, D. Kremp, M. Schlanges, W.D. Kraeft, Quantum Kinetic Theory for Laser Plasmas. Dynamical Screening in Strong Fields, *Contrib. Plasma Phys.* **39**, 329 (1999)
32. M. Bonitz, D. Kremp, D.C. Scott, R. Binder, W.D. Kraeft, H.S. Köhler, Numerical analysis of non-Markovian effects in charge-carrier scattering: one-time versus two-time kinetic equations, *J. Phys.: Condens. Matter* **8**, 6057 (1996)
33. K. Balzer, M. Bonitz, *Nonequilibrium Green's Function Approach to Inhomogenous Systems, Lec. Notes in Phys.* 867 (Springer, Berlin, 2013)
34. L.P. Kadanoff, G. Baym, *Quantum Statistical Mechanics* (W.A. Benjamin, New York 1962)
35. N.-H. Kwong, M. Bonitz, Real-Time Kadanoff-Baym Approach to Plasma Oscillations in a Correlated Electron Gas, *Phys. Rev. Lett.* **84**, 1768 (2000)
36. D. Kremp, M. Schlanges, W.D. Kraeft, *Quantum Statistics of Nonideal Plasmas* (Springer, Berlin, 2005)
37. M. Bonitz et al., Theory and simulations of strong correlations in quantum Coulomb systems, *J. Phys. A: Math. Gen.* **36**, 5921 (2003)
38. M. Bonitz, J.W. Dufty, Quantum kinetic theory of metal clusters in an intense electromagnetic field I, *Cond. Matt. Phys.* **7**, 483 (2004)
39. M. Bonitz et al., Classical and quantum Coulomb crystals, *Phys. Plasmas* **15**, 055704 (2008)
40. M. Bonitz, Kinetic theory for quantum plasmas, *AIP Conf. Proc.* **1421**, 135 (2012)
41. S. Ichimaru, Strongly coupled plasmas: high-density classical plasmas and degenerate electron liquids, *Rev. Mod. Phys.* **54**, 1017 (1982)
42. P.K. Shukla, B. Eliasson, Colloquium: Nonlinear collective interactions in quantum plasmas with degenerate electron fluids, *Rev. Mod. Phys.* **83**, 885 (2011)
43. S.V. Vladimirov, Y.O. Tyshetskiy, On description of collisionless quantum plasmas, *Phys. Uspekhi* **54**, 1243 (2011)
44. E. Madelung, Quantum theory in hydrodynamic form (in German), *Z. Physik* **40**, 322 (1927)
45. G. Manfredi, How to model quantum plasmas, *Fields Inst. Commun.* **46**, 263 (2005)
46. G. Manfredi, F. Haas, Self-consistent fluid model for a quantum electron gas, *Phys. Rev. B* **64**, 075316 (2001)
47. G. Manfredi, P.-A. Hervieux, Y. Yin, N. Crouseilles, Collective Electron Dynamics in Metallic and Semiconductor Nanostructures, In: *Atomic-Scale Modeling of Nanosystems and Nanostructured Materials, Lec. Notes Phys.* 795 (Springer, Berlin, 2010)
48. N. Crouseilles, P.-A. Hervieux, G. Manfredi, Quantum hydrodynamic Models for nonlinear electron dynamics in thin metal films, *Phys. Rev. B* **78**, 155412 (2008)
49. F. Haas, *Quantum Plasmas-An Hydrodynamic Approach* (Springer, New York, 2011)
50. A. Jüngel, *Transport equations in Semiconductors* (Springer, Berlin, 2009)
51. C.L. Gardner, The Quantum Hydrodynamic Model for Semiconductor Devices, *SIAM (Soc. Ind. Appl. Math.) J. Appl. Math.* **54**, 409 (1994)
52. A. Bennett, Influence of the Electron Charge Distribution on Surface-Plasmon Dispersion, *Phys. Rev. B* **1**, 203 (1970)
53. M. Marklund, G. Brodin, L. Stenflo, C.S. Liu, New quantum limits in plasmonic devices, *Euro. Phys. Lett.* **84**, 17006 (2008)
54. E.P. Gross, Structure of a quantized vortex in boson system, *Nuovo Cimento* **20**, 454 (1961)
55. L.P. Pitaevskii, Vortex Lines in an Imperfect Bose Gas, *Zh. Eksp. Teor. Fiz.* **40**, 646 (1961) [*Sov. Phys. JETP* 13, 451 (1961)]
56. A. Serbeto, L.F. Monteiro, K.H. Tsui, J.T. Mendonca, Quantum plasma fluid model for high-gain free-electron lasers, *Plasma Phys. Control. Fusion* **51**, 124024 (2009)
57. A. Kendl, P.K. Shukla, Drift wave turbulence in a dense semi-classical magnetoplasma, *Phys. Lett. A* **375**, 3138 (2011)



58. D. Bohm, A Suggested Interpretation of the Quantum Theory in Terms of "Hidden" Variables. I, Phys. Rev. 85, **166** (1952)
59. D. Bohm, A Suggested Interpretation of the Quantum Theory in Terms of "Hidden" Variables. II, Phys. Rev. 85, **180** (1952)
60. D. Bohm, J.P. Vigier, Model of the Causal Interpretation of Quantum Theory in Terms of a Fluid with Irregular Fluctuations. Phys. Rev. **96**, 208 (1954)
61. P.R. Holland, *The Quantum Theory of Motion* (Cambridge, New York, 1993)
62. R.E. Wyatt, *Quantum Dynamics with Trajectories* (Springer, Berlin, 2005)
63. E.P. Wigner, On the Quantum Correction for Thermodynamic Equilibrium, Phys. Rev. **40**, 749 (1932)
64. J.E. Moyal, Quantum mechanics as a statistical theory, Proc. Cambridge Phil. Soc. **45**, 99 (1949)
65. P. Carruthers, F. Zachariasen, Quantum collision theory with phase-space distributions, Rev. Mod. Phys. **55**, 245 (1983)
66. M. Hillery, R.F. O'Connell, M.O. Scully, E.P. Wigner, Distribution functions in physics: Fundamentals, Phys. Rep. **106**, 121 (1984)
67. H.W. Lee, Theory and Application of the Quantum Phase-Space Distribution-Functions, Phys. Rep., **259**, 147 (1995)
68. J. Dawson, On Landau Damping, Phys. Fluid **4**, 869 (1961)
69. F. Haas, G. Manfredi, M. Feix, Multistream model for quantum plasma, Phys. Rev. E **62**, 2763 (2000)
70. M. Bonitz, E. Pehlke, T. Schoof, Attractive forces between ions in quantum plasmas: Failure of linearized quantum hydrodynamics, Phys. Rev. E **87**, 033105 (2013)
71. J. Lindhard, K. Dan. Vidensk. Selsk. Mat. Fys. Medd. **28**, 8 (1954)
72. V.O. Golubnychiy, M. Bonitz, D. Kremp, M. Schlanges, Dynamical properties of plasmon dispersion of a weakly degenerate correlated one-component plasma, Phys. Rev. E **64**, 016409 (2001)
73. D.M. Melrose, *Quantum Plasmadynamics: Unmagnetized plasmas, Lec. Notes in Phys 735* (Springer, New York, 2008)
74. D.B. Melrose, A. Mushtaq, Quantum recoil and Bohm diffusion, Phys. Plasmas **16**, 094508 (2009)
75. M. Bonitz, Impossibility of plasma instabilities in isotropic quantum plasmas, Phys. Plasmas **1**, 832 (1994)
76. W.R. Frensley, Boundary conditions for open quantum systems driven far from equilibrium, Rev. Mod. Phys. **62**, 745 (1990)
77. A.F. Alexandrov, L.S. Bogdankevich, A.A. Rukhadze, Osnovy Elektrodinamiki Plazmy (*Principles of Plasma Electrodynamics*) (Moscow: Vysshaya Shkola, 1988) [Translated into English (Springer, Berlin, 1984)]
78. F. Haas, L.G. Garcia, J. Goedert, G. Manfredi, Quantum ion-acoustic waves, Phys. Plasmas **10**, 3858 (2003)
79. F. Haas, A. Bret, Nonlinear low frequency collisional quantum Buneman instability, Europhys. Lett. **97**, 26001 (2012)
80. O. Buneman, Dissipation of Currents in Ionized Media, Phys. Rev. **115**, 503 (1959)
81. S. Bauch et al., Introduction to Quantum Plasma Simulations, Chapter in: *Introduction to Complex Plasmas*. M. Bonitz, N. Horing, and P. Ludwig (eds.), (Springer, Berlin, 2010)
82. V.E. Zakharov, Collapse of Langmuir waves, Sov. Phys. JETP **35**, 908 (1972)
83. L.G. Garcia, F. Haas, L. de Oliveira, J. Goedert, Modified Zakharov equations for plasmas with a quantum correction, Phys. Plasmas **12**, 012302 (2005)
84. F. Haas, P.K. Shukla, Quantum and classical dynamics of Langmuir wave packets, Phys. Rev. E **79**, 066402 (2009)
85. S.A. Khan, H. Saleem, Linear coupling of Alfvén waves and acoustic-type modes in dense quantum magnetoplasmas, Phys. Plasmas **16**, 052109 (2009)
86. H. Saleem, Ali Ahmad, S.A. Khan, Low frequency electrostatic and electromagnetic modes of ultracold magnetized nonuniform dense plasmas, Phys. Plasmas **15**, 094501 (2008)

87. B. Shokri, A.A. Rukhadze, Quantum drift waves, *Phys. Plasmas* **6**, 4467 (1999)
88. P.K. Shukla, B. Eliasson, Novel Attractive Force between Ions in Quantum Plasmas, *Phys. Rev. Lett.* **108**, 165007 (2012); Erratum: *Phys. Rev. Lett.* **108**, 219902 (2012); Erratum: *Phys. Rev. Lett.* **109**, 019901 (2012)
89. P.K. Shukla, B. Eliasson, M. Akbari-Moghanjoughi, Comment on "Attractive forces between ions in quantum plasmas: Failure of linearized quantum hydrodynamics", *Phys. Rev. E* **87**, 037101 (2013)
90. M. Bonitz, E. Pehlke, T. Schoof, Reply to "Comment on Attractive forces between ions in quantum plasmas: Failure of linearized quantum hydrodynamics", *Phys. Rev. E* **87**, 037102 (2013)
91. M. Bonitz, E. Pehlke, T. Schoof, Comment on "Discussion on Novel attractive force between ions in quantum plasmas—failure of simulations based on a density functional approach", accepted for publication in *Phys. Scripta* (2013); arXiv:1309.5897
92. M. Marklund, G. Brodin, Dynamics of Spin- $\frac{1}{2}$  quantum plasmas, *Phys. Rev. Lett.* **98**, 025001 (2007)
93. S.M. Mahajan, F. Asenjo, Vortical dynamics of spinning quantum plasma: helicity conservation, *Phys. Rev. Lett.* **107**, 195003 (2011)
94. S. Braun, F. Asenjo, S.M. Mahajan, Spin-Gradient-Driven Light Amplification in a quantum plasma, *Phys. Rev. Lett.* **109**, 175003 (2012)
95. G.S. Krishnaswami, R. Nityananda, A. Sen, A. Tyagaraja, A critique of recent theories of spin half quantum plasmas, arXiv:1306.1774 (2013)
96. E.M. Lifshitz, L.P. Pitaevski, *Physical Kinetics* (Pergamon, Oxford, 1981)
97. N.W. Ashcroft, N.D. Mermin, *Solid State Physics* (Harcourt Brace, New York, 1976)
98. C. Kittel, *Introduction to Solid State Physics* (John Wiley, New York, 1963)